

Low Energy antikaon-nucleon/nuclei interaction studies by AMADEUS



Meson2018

15th International Workshop on Meson Physics
KRAKÓW, POLAND
7th - 12th June 2018

Kristian Piscicchia*

Laboratori Nazionali di Frascati (INFN)
Centro Fermi

Museo Storico della Fisica e Centro Studi e Ricerche Enrico Fermi

kristian.piscicchia@lnf.infn.it

Low-energy QCD in the u-d-s sector

Investigation of **in-medium modification of the $\bar{K}N$ interaction** fundamental for the low-energy QCD in the non perturbative regime.

Chiral perturbation theory (ChPT): effective field theory where mesons and baryons represent the effective degrees of freedom instead of the fundamental quark and gluon fields.

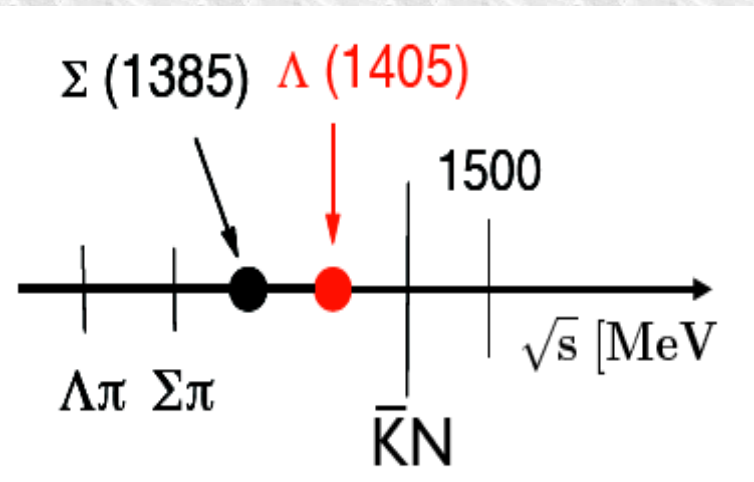
$$\mathcal{L}_{eff} = \mathcal{L}_{mesons}(\Phi) + \mathcal{L}_B(\Phi, \Psi_B)$$

- chiral symmetry is **spontaneously broken** \rightarrow existence of massless and spinless Nambu-Goldstone bosons which are identified with the pions (SU(2)). Explicitly broken by quark masses.
- **very successful** in describing the πN , $\pi\pi$ and NN interactions in the low-energy regime.

Problematic extension of the theory to the s sector, not directly applicable to the $\bar{K}N$ channel.

Low-energy QCD in the u-d-s sector

ChPT not applicable to the $\bar{K}N$ channel due to the emerging of the $\Lambda(1405)$ and the $\Sigma(1385)$ resonances just below the $\bar{K}N$ mass threshold (~ 1432 MeV)



- $\Lambda(1405)$ $I=0$ $J^P = \frac{1}{2}^-$
 $M = (1405.1^{+1.3}_{-1.0})$ MeV $\Gamma = (50.5 \pm 2.0)$ MeV
 decay modes: $\Sigma\pi$ ($I=0$) 100%
- $\Sigma(1385)$ $I=1$ $J^P = \frac{3}{2}^+$
 decay modes: $\Lambda\pi$ ($I=1$) $(87.0 \pm 1.5)\%$
 $\Sigma\pi$ ($I=1$) $(11.7 \pm 1.5)\%$

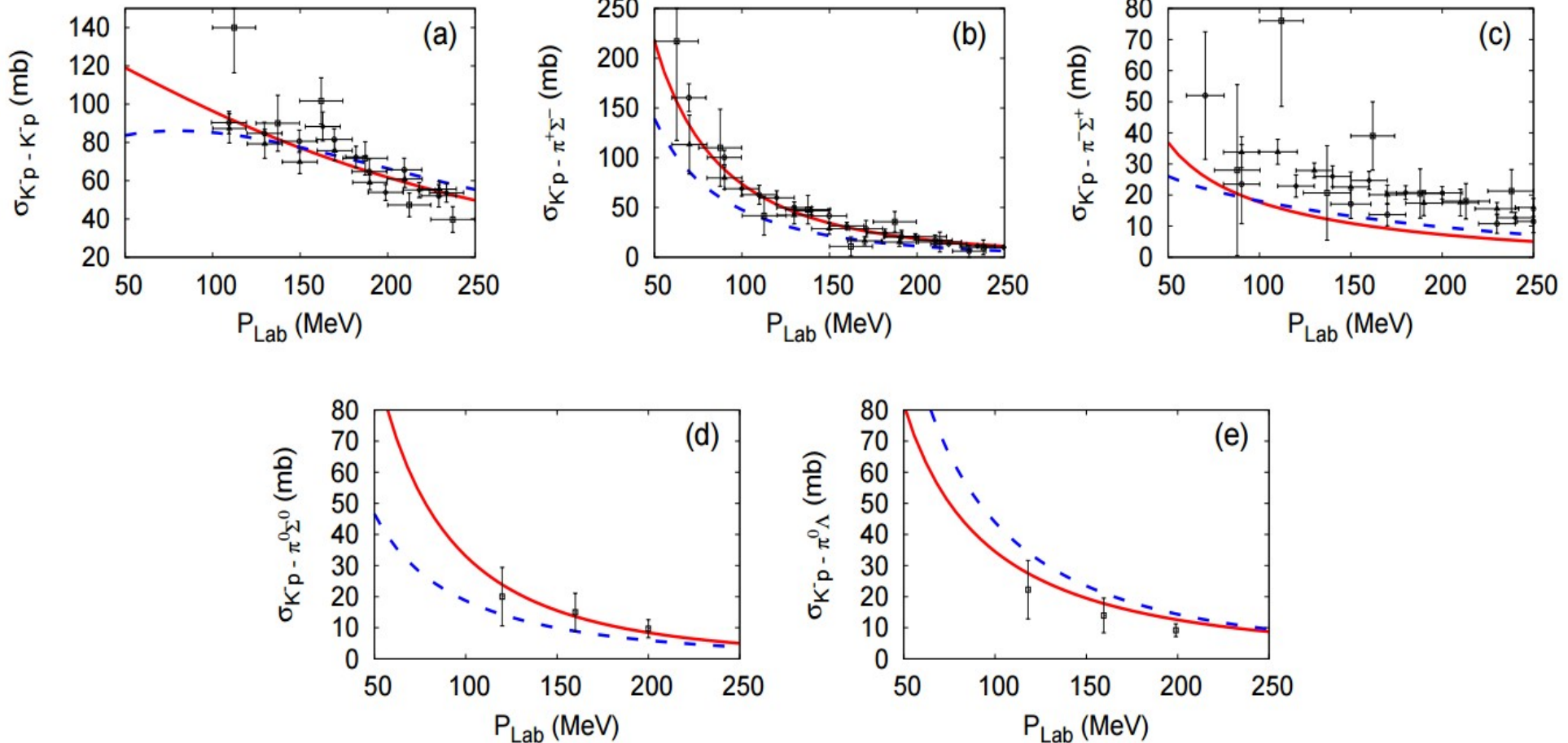
Possible solutions:

- Non-perturbative Coupled Channels approach: Chiral Unitary SU(3) Dynamics
 - Phenomenological $\bar{K}N$ and NN potentials

Low-energy QCD in the u-d-s sector

The parameters of the models are constrained by the existing scattering data → above the threshold

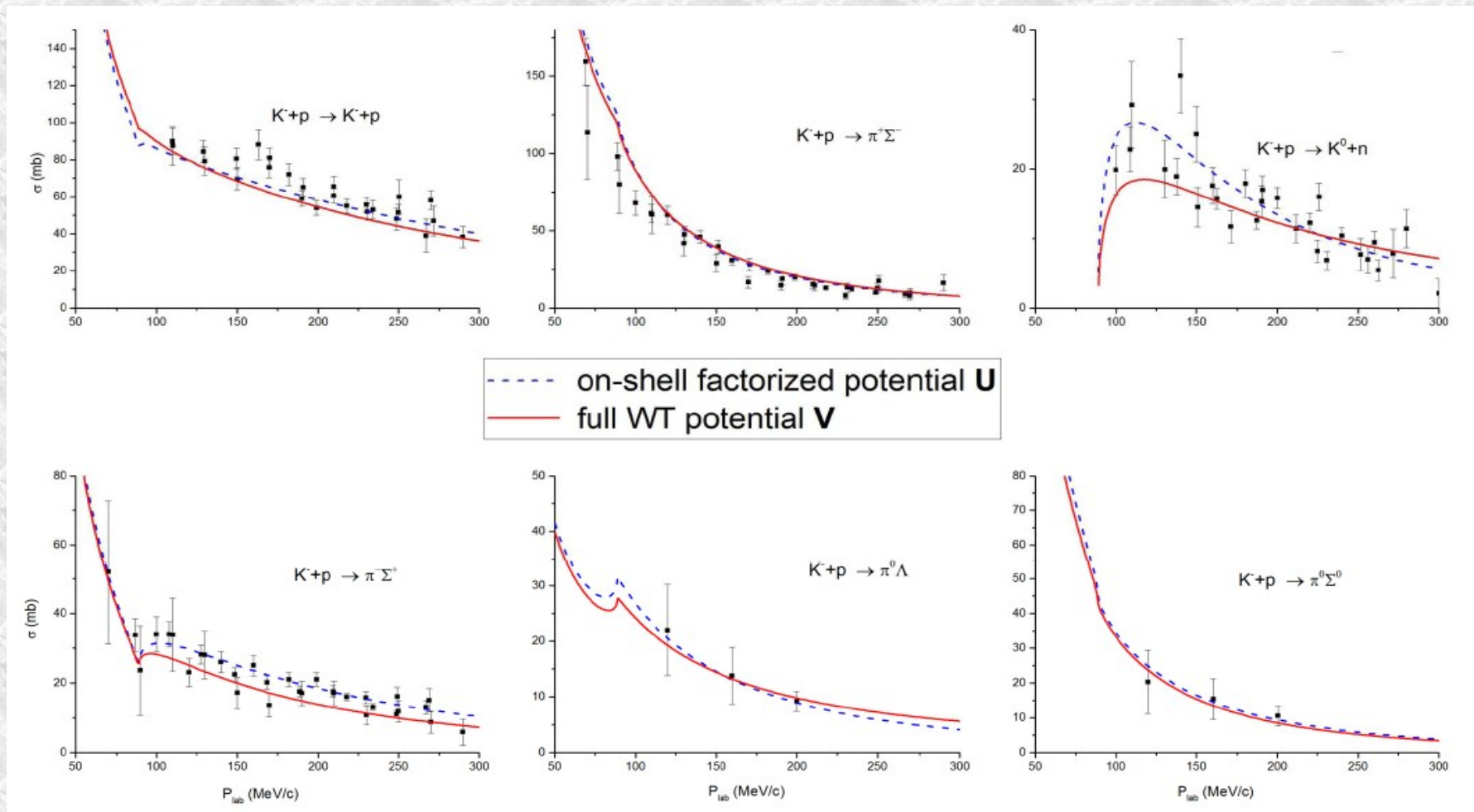
- Phen. [Y. Ikeda and T. Sato, Phys. Rev. C76, 035203 (2007)]
 - Chiral [S. Ohnishi, Y. Ikeda, T. Hyodo, W. Weise, Phys.Rev. C93 (2016) no.2, 025207]
- also see the talk



Low-energy QCD in the u-d-s sector

The parameters of the models are constrained by the existing scattering data → [above the threshold](#)

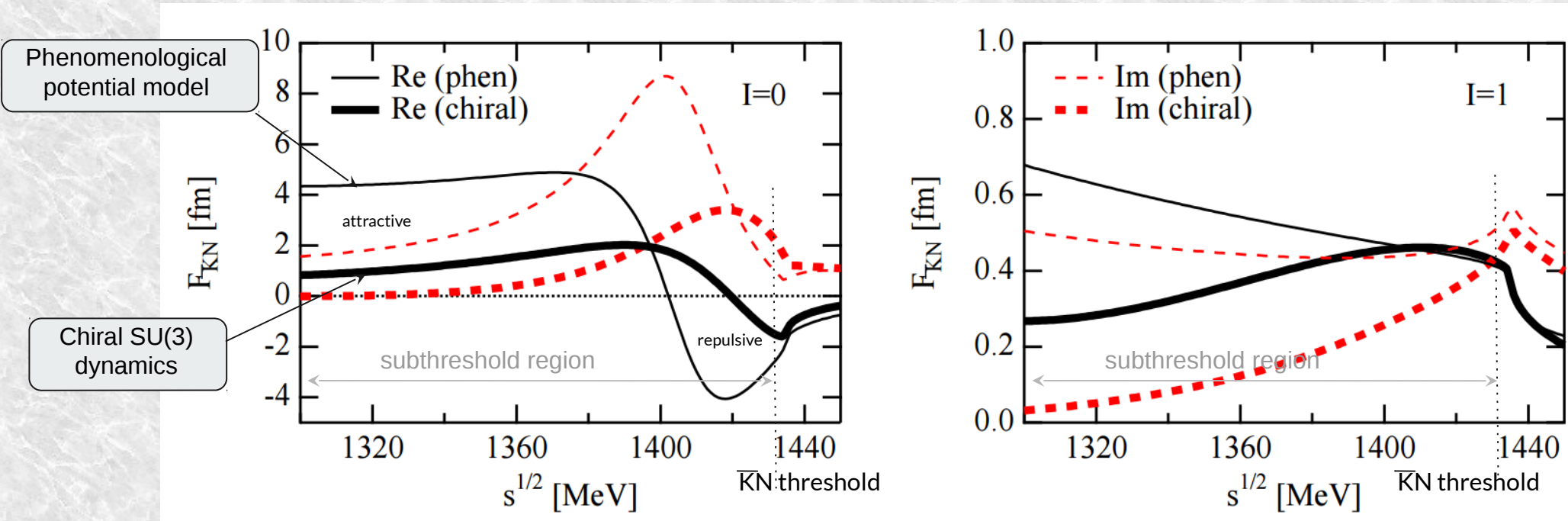
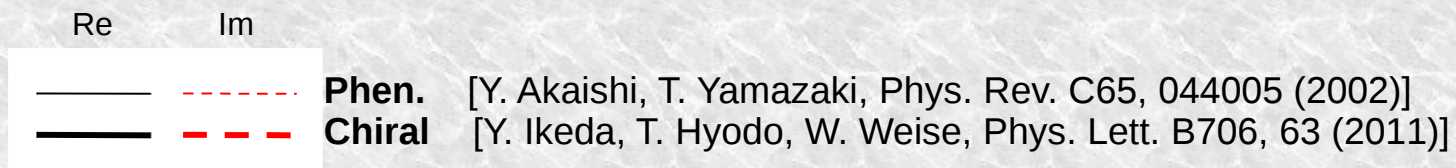
Chiral J. Révai [Few Body Systems 59(2018)49] → also [see the talk](#)



Low-energy QCD in the u-d-s sector

...but... large differences in the subthreshold extrapolations!

Significantly weaker attraction in chiral SU(3) models than in phenomenological potential models.



The $\Lambda(1405)$ case

- Chiral unitary models: $\Lambda(1405)$ is an $I = 0$ quasibound state emerging from the coupling between the $\bar{K}N$ and the $\Sigma\pi$ channels. Two poles in the neighborhood of the $\Lambda(1405)$:

two poles: about 1420 ; about = 1380 MeV

Phys. Lett. B 500 (2001), Phys. Rev. C 66 (2002), (Nucl. Phys. A 725(2003) 181) .. many others .. (Nucl. Phys. A881, 98 (2012)) .. others

mainly coupled to $\bar{K}N$

mainly coupled to $\Sigma\pi$

→ line-shape depends on production mechanism

- Akaishi-Esmaili-Yamazaki phenomenological potential

Phys. Lett. B 686 (2010) 23-28 Confirmation of single pole ansatz?

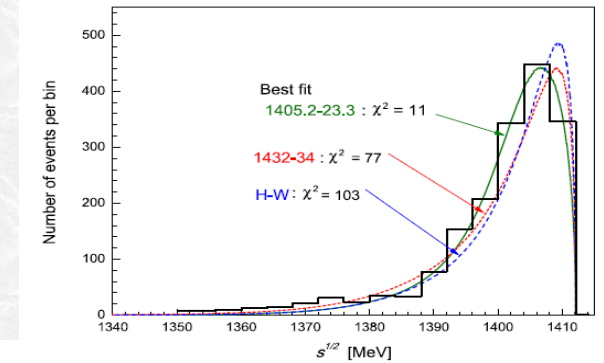
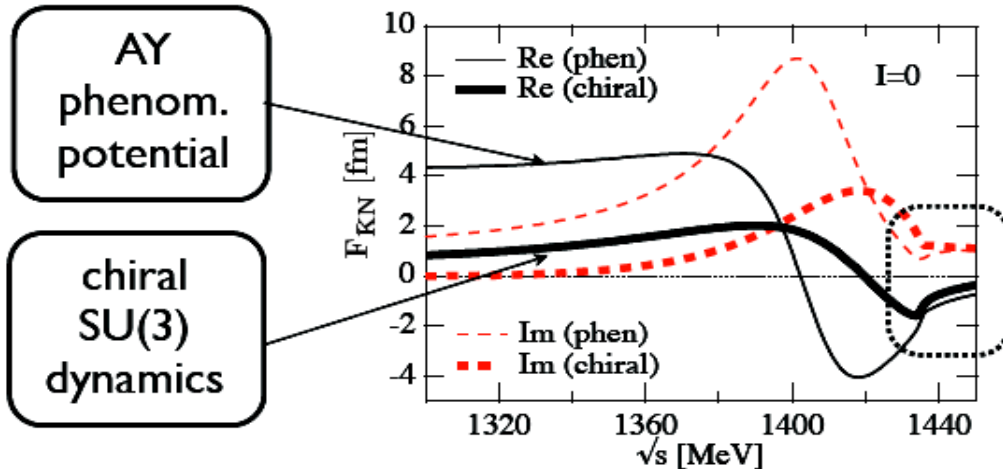
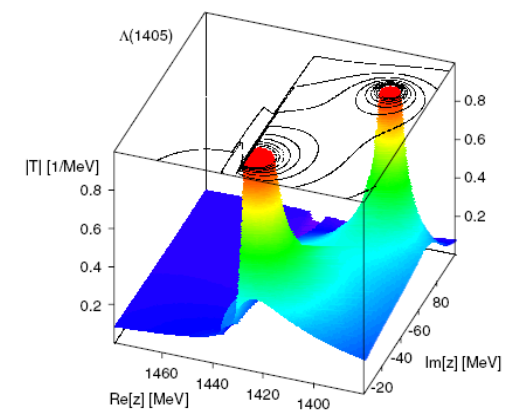


Fig. 6. Detailed differences in $M_{\Sigma\pi}$ spectra among the Hyodo-Weise prediction and the present model predictions.



large differences in subthreshold extrapolations



- Chiral dynamics predicts significantly weaker attraction than AY (local, energy independent) potential in far-subthreshold region

The $\Lambda(1405)$ case

- Chiral unitary models: $\Lambda(1405)$ is an $I = 0$ quasibound state emerging from the coupling between the $\bar{K}N$ and the $\Sigma\pi$ channels. Two poles in the neighborhood of the $\Lambda(1405)$:

two poles: about 1420 ; about = 1380 MeV

Phys. Lett. B 500 (2001), Phys. Rev. C 66 (2002), (Nucl. Phys. A 725(2003) 181) .. many others .. (Nucl. Phys. A881, 98 (2012)) .. others

mainly coupled to $\bar{K}N$

mainly coupled to $\Sigma\pi$

→ line-shape depends on production mechanism

- J. Révai [Few Body Systems 59(2018)49]: solving the LS equation with full WT potential → low mass pole in the $\bar{K}N - \Sigma\pi$ system disappears

Pole positions (MeV):

	z_1	z_2
U	1428 - 35 i	1384 - 62 i
V	1425 - 21 i	-

The $\Lambda(1405)$ case

BUBBLE CHAMBER search of the $\Lambda(1405)$:

- O. Braun et al. Nucl. Phys. B129 (1977) 1

K⁻ induced reactions on d $\rightarrow \Sigma^- \pi^+ n$ the resonance is found & 1420 MeV

- D. W. Thomas et al., Nucl. Phys. B56 (1973) 15

pion induced reaction $\pi^- p \rightarrow K^+ \pi^- \Sigma$ the resonance is found & 1405 MeV

- R. J. Hemingway, Nucl. Phys. B253 (1985) 742

K⁻ p $\rightarrow \pi^- \Sigma^+(1660) \rightarrow \pi^- (\pi^+ \Lambda(1405)) \rightarrow \pi^- \pi^+ (\pi \Sigma)$ & 4.2 GeV

analysed by Dalitz and Deloff $M = 1406.5 \pm 4.0$ MeV, $\Gamma = 50 \pm 2$ MeV

- HADES coll. Phys. Rev. C 87, 025201 (2013)

pp $\rightarrow p K^+ \pi^- \Sigma$ the resonance is found & 1390 MeV

The $\Lambda(1405)$ case

THE “LINE-SHAPE” OF THE $\Lambda(1405)$ DEPENDS ON THE OBSERVED CHANNEL !!

$$\frac{d\sigma(\Sigma^-\pi^+)}{dM} \propto \frac{1}{3} |T^0|^2 + \frac{1}{2} |T^1|^2 + \frac{2}{\sqrt{6}} \text{Re}(T^0 T^{1*})$$

$$\frac{d\sigma(\Sigma^+\pi^-)}{dM} \propto \frac{1}{3} |T^0|^2 + \frac{1}{2} |T^1|^2 - \frac{2}{\sqrt{6}} \text{Re}(T^0 T^{1*})$$

$$\frac{d\sigma(\Sigma^0\pi^0)}{dM} \propto \frac{1}{3} |T^0|^2$$

The $\Lambda(1405)$ case

THE “LINE-SHAPE” OF THE $\Lambda(1405)$ DEPENDS ON THE OBSERVED CHANNEL !!

$$\frac{d\sigma(\Sigma^-\pi^+)}{dM} \propto \frac{1}{3}|T^0|^2 + \frac{1}{2}|T^1|^2 + \frac{2}{\sqrt{6}}\text{Re}(T^0T^{1*})$$

$$\frac{d\sigma(\Sigma^+\pi^-)}{dM} \propto \frac{1}{3}|T^0|^2 + \frac{1}{2}|T^1|^2 - \frac{2}{\sqrt{6}}\text{Re}(T^0T^{1*})$$

$$\frac{d\sigma(\Sigma^0\pi^0)}{dM} \propto \frac{1}{3}|T^0|^2$$

IS DIFFERENT IN $\Sigma^+\pi^-$ VS $\Sigma^-\pi^+$
DUE TO ISOSPIN INTERFERENCE

The $\Lambda(1405)$ case

THE “LINE-SHAPE” OF THE $\Lambda(1405)$ DEPENDS ON THE OBSERVED CHANNEL !!

$$\frac{d\sigma(\Sigma^-\pi^+)}{dM} \propto \frac{1}{3}|T^0|^2 + \frac{1}{2}|T^1|^2 + \frac{2}{\sqrt{6}}\text{Re}(T^0T^{1*})$$

$$\frac{d\sigma(\Sigma^+\pi^-)}{dM} \propto \frac{1}{3}|T^0|^2 + \frac{1}{2}|T^1|^2 - \frac{2}{\sqrt{6}}\text{Re}(T^0T^{1*})$$

$$\frac{d\sigma(\Sigma^0\pi^0)}{dM} \propto \frac{1}{3}|T^0|^2$$

IS DIFFERENT IN $\Sigma^+\pi^-$ VS $\Sigma^-\pi^+$

DUE TO ISOSPIN INTERFERENCE

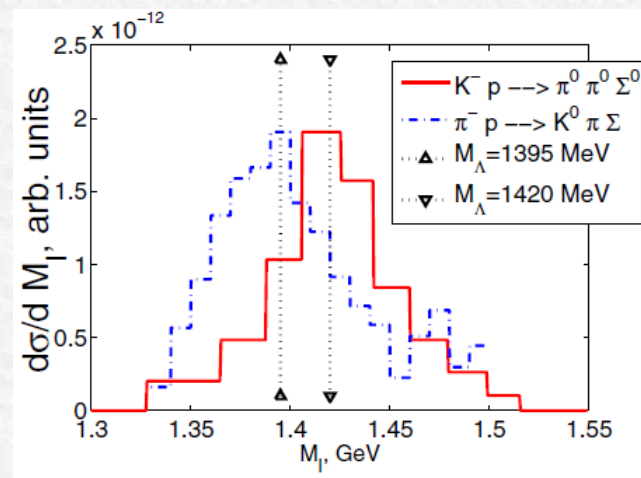
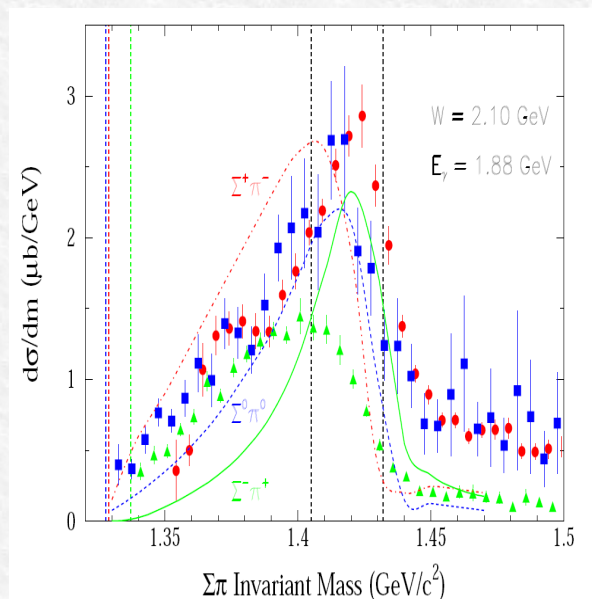
THE CLEANEST SIGNATURE OF THE $\Lambda(1405)$ IS GIVEN BY THE NEUTRAL CHANNEL:

- is free from isospin interference
- is purely $I = 0$, no $\Sigma(1385)$ contamination.

$\Lambda(1405)$.. the golden channel

Crystall Ball: $K^- p \rightarrow \Sigma^0 \pi^0 \pi^0$ for kaon momentum in the range (514-750 MeV/c). S. Prakhov et al. Phys Rev. C70 (2004) 03465

(interpreted by Magas et al. PRL 95, 052301 (2005))



CLAS: $\gamma p \rightarrow K^+ \Sigma \pi$

AIP Conf.Proc. 1441 (2012) 296-298

COSY julich: $pp \rightarrow pK^+ \Sigma^0 \pi^0$

(I. Zychor et al., Phys. Lett. B 660 (2008) 167)

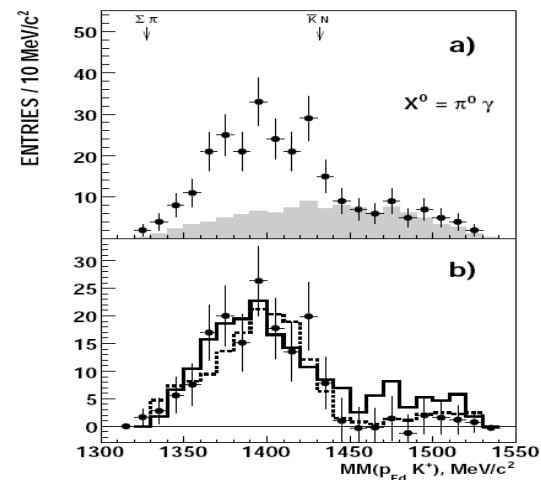


Fig. 4. a) Missing-mass $MM(p_{Fd}K^+)$ distribution for the $pp \rightarrow pK^+ p\pi^- X^0$ reaction for events with $M(p_{sd}\pi^-) \approx m(\Lambda)$ and $MM(pK^+ p\pi^-) > 190 \text{ MeV}/c^2$. Exper-

The $\Lambda(1405)$ case

Two main **biases**:

- the **kinematical energy threshold 1412 MeV**
($M_K + M_p - |BE_p|$) the high pole energy region is closed,
- The **shape and the amplitude of the NON-RESONANT $\Sigma\pi$ production** below $K\bar{p}N$ threshold is unknown.

An ideal experiment:

- $\Lambda(1405)$ is produced in $K^- p$ absorption \rightarrow mainly coupled to the high mass pole,
- $\Lambda(1405)$ is observed in the $\Sigma^0\pi^0$ decay channel (pure isospin 0),
- K^- is absorbed in-flight on a bound proton with $p_K \sim 100$ MeV, $\Sigma\pi$ invariant mass gain of ~ 10 MeV to open an energy window to the high mass pole.
- Knowledge of the $\Sigma\pi$ NON-RESONANT production amplitude ... a choice of the resonant amplitude necessary to model simulations

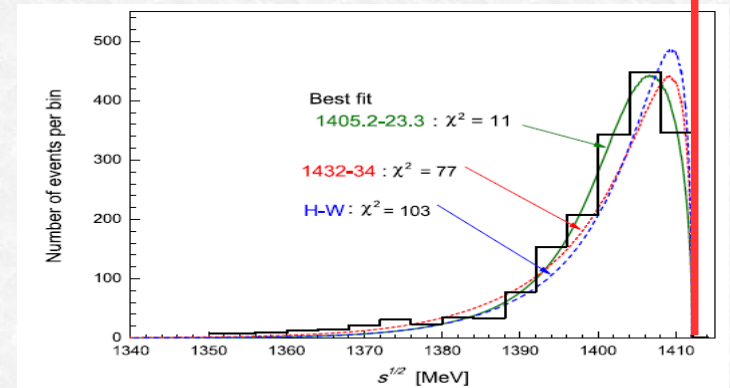
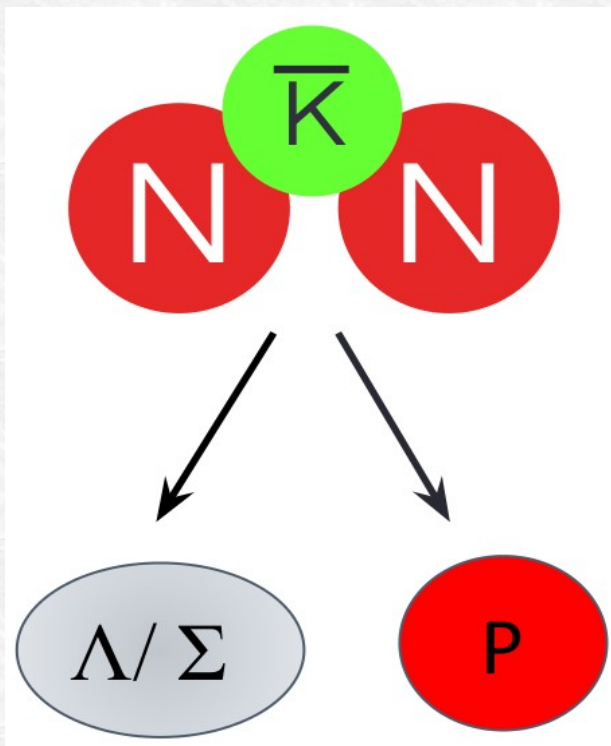


Fig. 6. Detailed differences in $M_{\Sigma\pi}$ spectra among the Hyodo-Weise prediction and the present model predictions.

How deep can an antikaon be bound in a nucleus?



Possible Bound States:

$$\begin{aligned} (K^- pp) &\rightarrow \Lambda p \\ &\rightarrow \Sigma^0 p \end{aligned}$$

$$\begin{aligned} (K^- ppn) &\rightarrow \Lambda d \\ &\rightarrow \Sigma^0 d \end{aligned}$$

predicted **if** strong $\bar{K}N$ interaction
in the $I=0$ channel.

[Wycech (1986) - Akaishi & Yamazaki (2002)]

K⁻pp bound state

....at the end of 2015

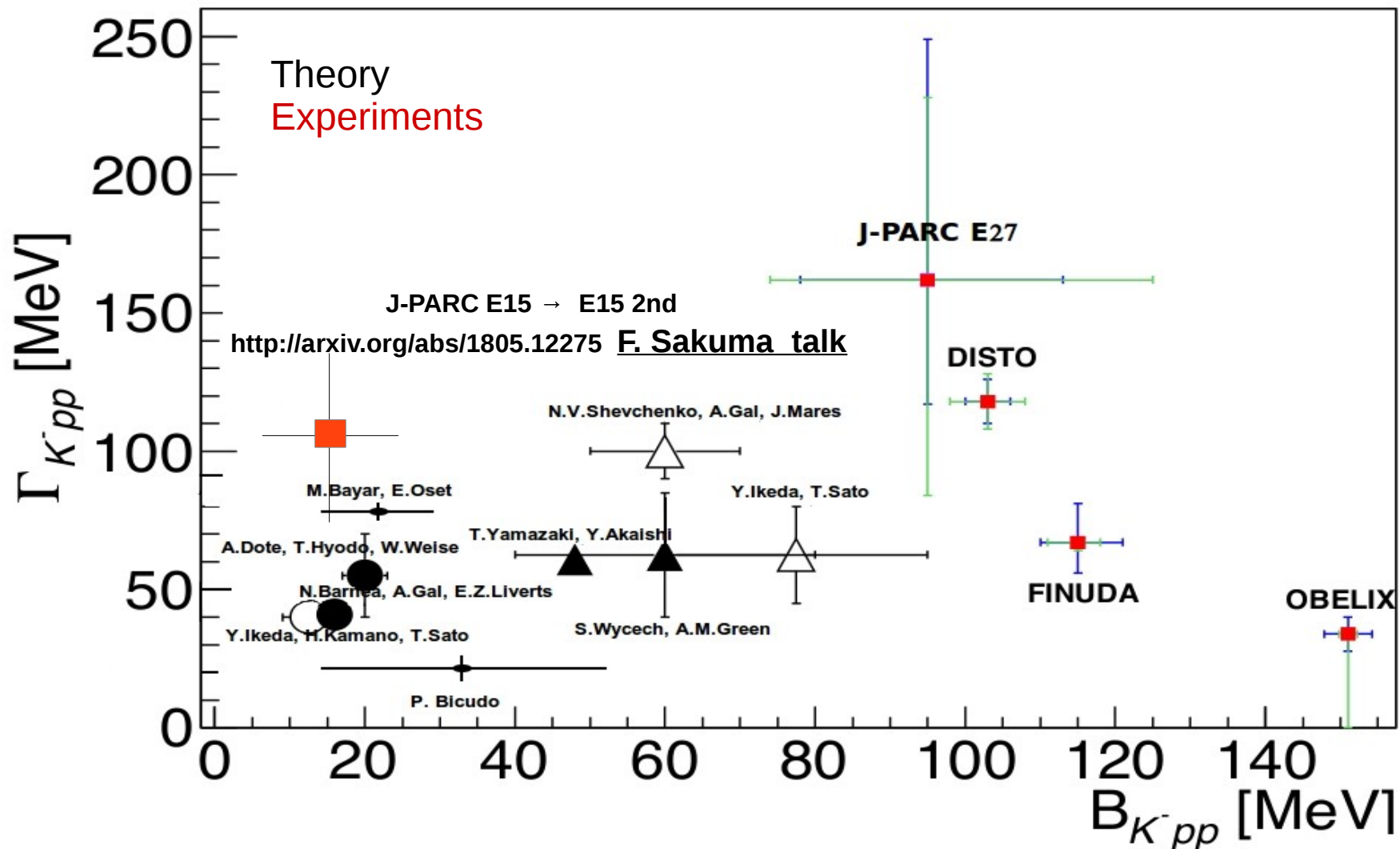
	BE (MeV)	Γ (MeV)	Reference
Dote, Hyodo, Weise	17-23	40-70	Phys.Rev.C79 (2009) 014003
Akaishi, Yamazaki	48	61	Phys.Rev.C65 (2002) 044005
Barnea, Gal, Liverts	16	41	Phys.Lett.B712 (2012) 132-137
Ikeda, Sato	60-95	45-80	Phys.Rev.C76 (2007) 035203
Ikeda, Kamano, Sato	9-16	34-46	Prog.Theor.Phys. (2010) 124(3): 533
Shevchenko, Gal, Mares	55-70	90-110	Phys.Rev.Lett.98 (2007) 082301
Revai, Shevchenko	32	49	Phys.Rev.C90 (2014) no.3, 034004
Maeda, Akaishi, Yamazaki	51.5	61	Proc.Jpn.Acad.B 89, (2013) 418
Bicudo	14.2-53	13.8-28.3	Phys.Rev.D76 (2007) 031502
Bayar, Oset	15-30	75-80	Nucl.Phys.A914 (2013) 349
Wycech, Green	40-80	40-85	Phys.Rev.C79 (2009) 014001

Experiments reporting DBKNS		
KEK-PS E549	T. Suzuki et al. MPLA23, 2520-2523 (2008)	
FINUDA	M. Agnello et al. PRL94, 212303 (2005)	Extraction of a signal
DISTO	T. Yamazaki et al. PRL104 (2010)	Extraction of a signal
OBELIX	G. Bendiscioli et al. NPA789, 222 (2007)	Extraction of a signal
HADES	G. Agakishiev et al. PLB742, 242-248 (2015)	Upper limit
LEPS/SPring-8	A.O. Tokiyasu et al. PLB728, 616-621 (2014)	Upper limit
J-PARC E15	T. Hashimoto et al. PTEP, 061D01 (2015)	Upper limit
J-PARC E27	Y. Ichikawa et al. PTEP, 021D01 (2015)	Extraction of a signal

How deep can an antikaon be bound in a nucleus?

interpreted in

T. Sekihara, E. Oset, A. Ramos, Prog. Theor. Exp. Phys (2016) (12): 123D03

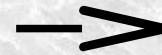
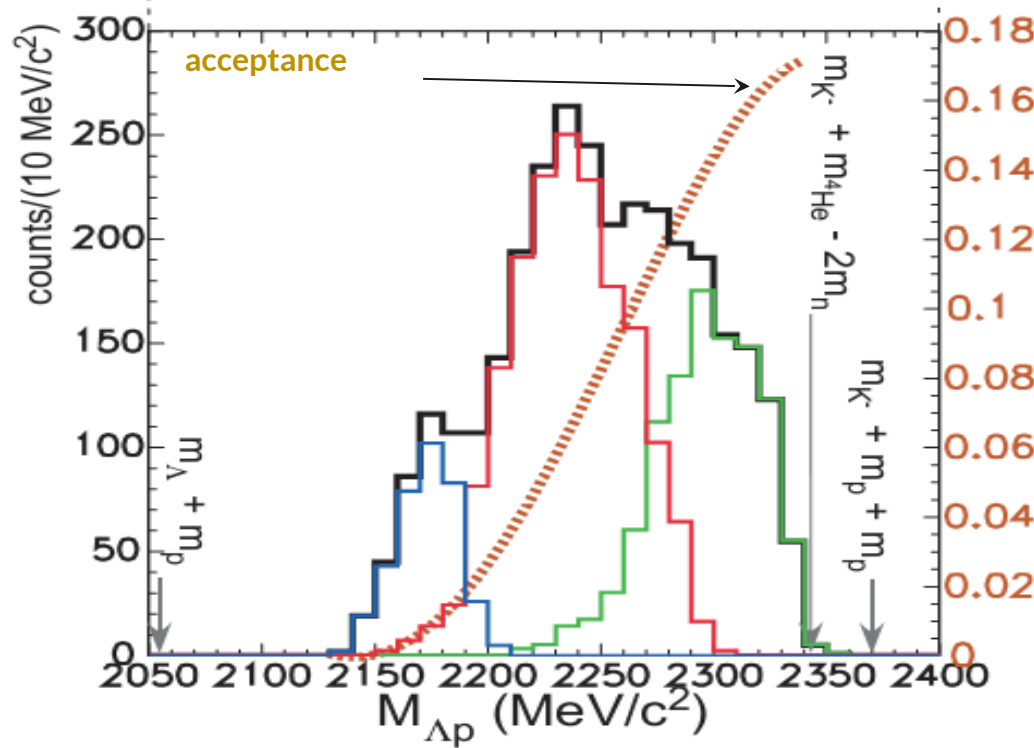


Bound state search in K⁻ induced reactions

E549 at KEK: $K^-_{\text{stop}} + {}^4\text{He} \rightarrow \Lambda + p + X'$

detected particles

[T. Suzuki et al., Mod. Phys. Lett. A23 (2008) 2520-2523.]

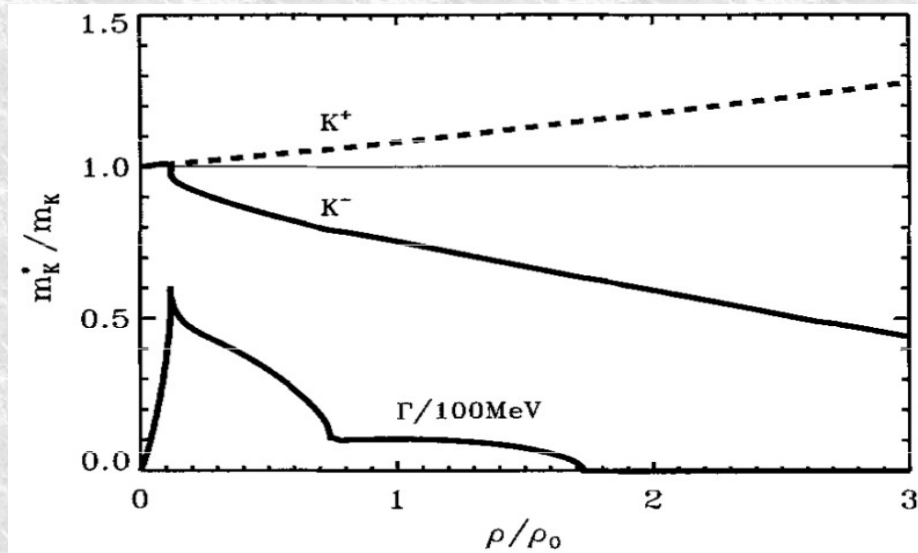


Measurement of yields and shapes of the K⁻ multi-nucleon yields is mandatory to solve the puzzle!

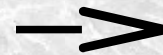
They are the counterpart of the non-resonant single nucleon capture

- **1NA**: K⁻ single nucleon absorption
- **2NA**: K⁻ two nucleon absorption
- **2NA + conversion, multi-nucleon, or Bound State?**

and K- multi-nucleon cross section?



Transport models and collision calculations need the measurement of the K- multi-nucleon cross sections at low energy



...

still missing!

In medium \bar{K} properties investigated in heavy-ion & proton nuclei collisions, K^- mass modification extrapolated from the K^- production yield

AMADEUS scientific case

- Nature of the $\Lambda(1405)$ & K-N amplitude below threshold → **$\Upsilon\pi$ CORRELATION STUDIES**

- K- multi-nucleons absorptions cross sections

- kaonic nuclear clusters

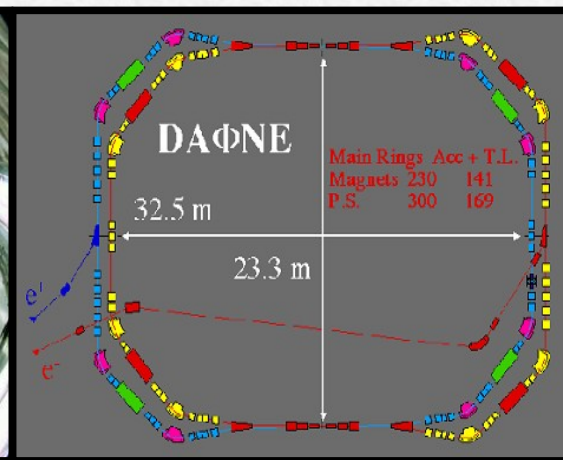
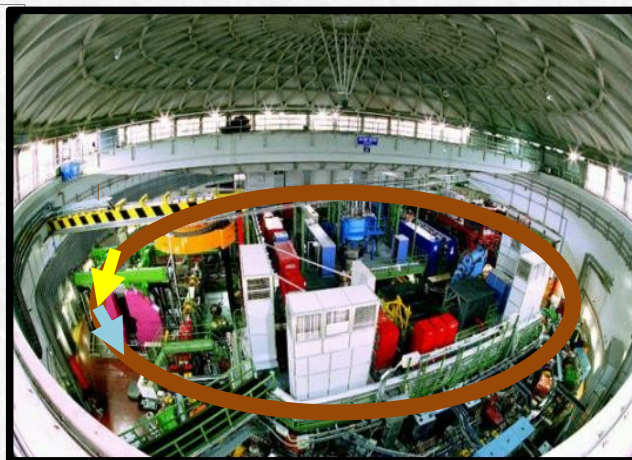
→ **YN CORRELATION STUDIES** (i.e. Λp , $\Sigma^0 p$, and Λt final states)

- Low-energy charged kaon **cross sections** for low momenta (100 MeV/c)
- YN scattering → extremely poor experimental information from scattering data
**(strong impact on the EoS of Neutron Stars
Related to NS merging radiation + GW emission)**

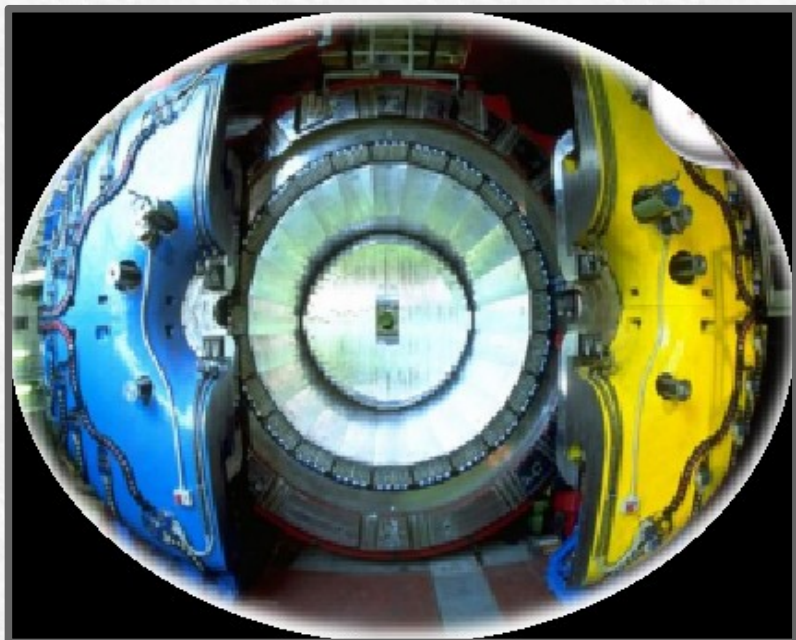
AMADEUS & DAΦNE

DAΦNE

- double ring e^+e^- collider working at C.M. energy of ϕ , producing $\approx 1000 \phi/s$
 - $\phi \rightarrow K^+K^-$ (BR = $(49.2 \pm 0.6)\%$)
 - **low momentum** Kaons $\approx 127 \text{ Mev}/c$
 - **back to back** K^+K^- topology



AMADEUS step 0 \rightarrow KLOE 2004-2005 dataset analysis ($\mathcal{L} = 1.74 \text{ pb}^{-1}$)



KLOE \rightarrow see talk by D. KISIELEWSKA

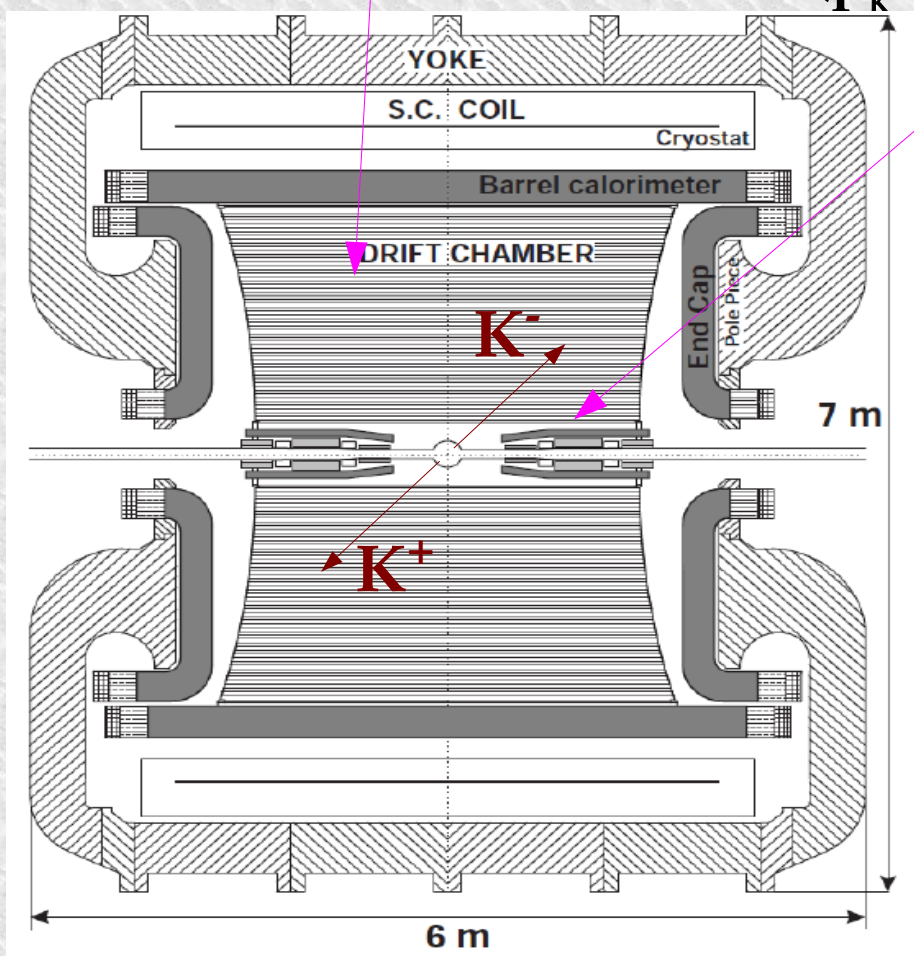
- Cylindrical drift chamber with a **4π geometry** and electromagnetic calorimeter
 - **96% acceptance**
- optimized in the energy range of all **charged particles** involved
- **good performance** in detecting **photons and neutrons** checked by kloNe group

[M. Anelli et al., Nucl Inst. Meth. A 581, 368 (2007)]₂₀

K⁻ absorption on light nuclei

from the materials of the KLOE detector
DC gas (90% He, 10% C₄H₁₀) & DC wall (C + H)

AT-REST (K⁻ absorbed from atomic orbit) or IN-FLIGHT
(p_K ~ 100 MeV)



Advantage:

excellent resolution ..

$$\sigma_{p\Lambda} = 0.49 \pm 0.01 \text{ MeV}/c \text{ in DC gas}$$

$$\sigma_{m\gamma\gamma} = 18.3 \pm 0.6 \text{ MeV}/c^2$$

Disadvantage:

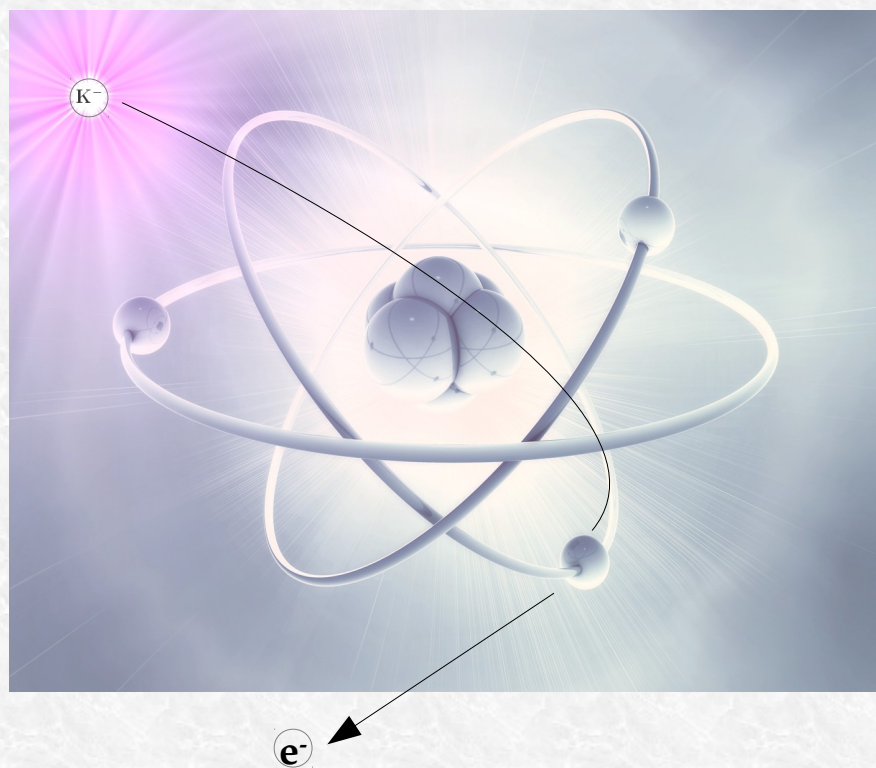
Not dedicated target → **different nuclei contamination** → complex interpretation .. but
→ **new features .. K⁻ in flight absorption.**

At-rest VS in-flight K^- captures

AT-REST

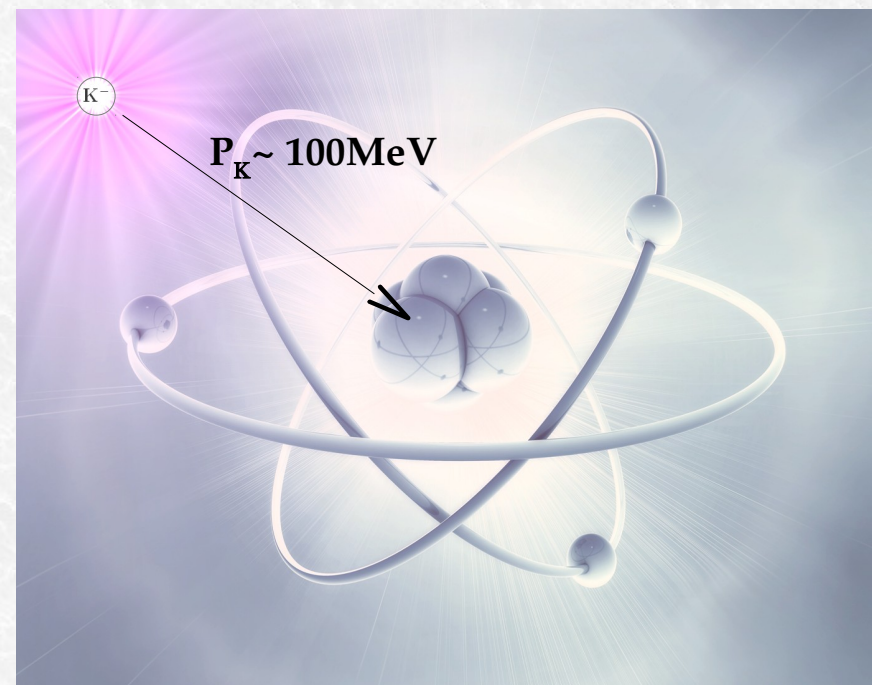
K^- absorbed from atomic orbit

($p_K \sim 0$ MeV)



IN-FLIGHT

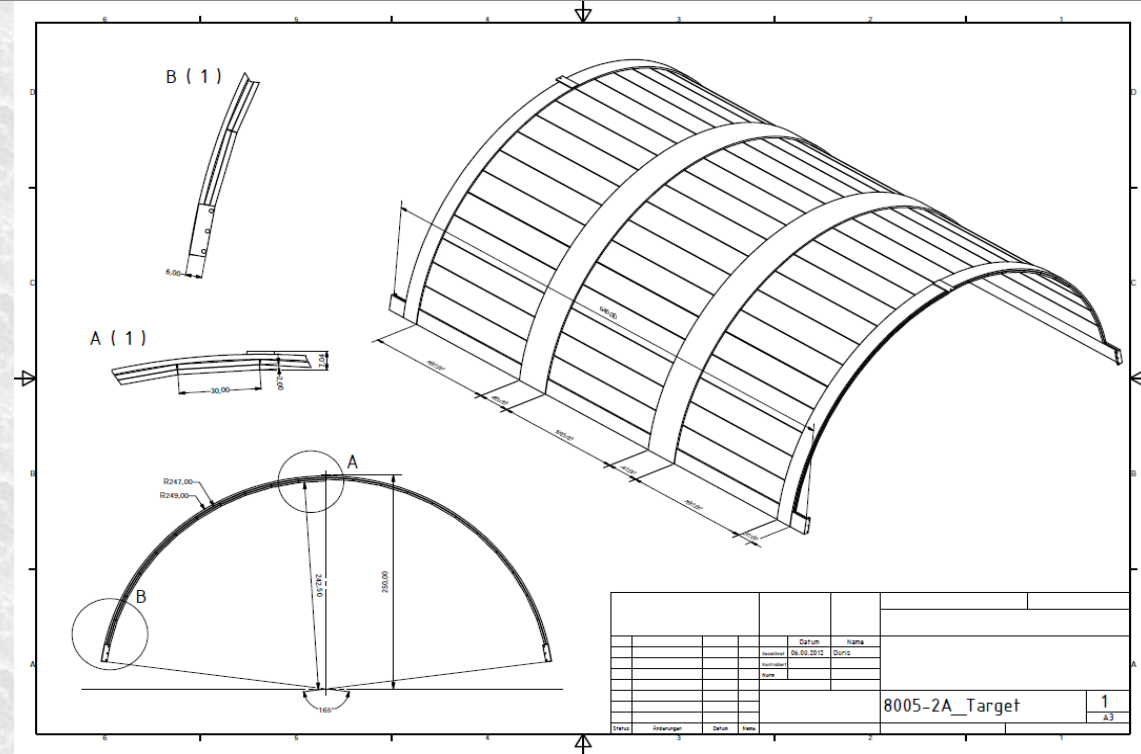
($p_K \sim 100$ MeV)



Pure graphite Carbon target

Advantages:

- gain in statistics
- pure K^- Carbon absorptions
- pure absorptions at-rest.



- MC simulation: 26% of K^- stopped in ^{12}C
- Thickness optimized to maximize the number of stopping K^- in the target (minimizing energy loss)

(~90 pb^{-1} ; analyzed 37 pb^{-1} , x 1.5 statistics)

K^- - N single nucleon absorption

resonant and non-resonant amplitudes

$\Lambda(1405)$ case

Phys.Rev.Lett.95:052301,2005

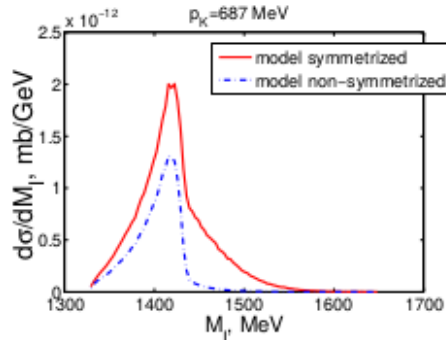


FIG. 4: Theoretical ($\pi^0\Sigma^0$) invariant mass distribution for an initial kaon lab momenta of 687 MeV. The non-symmetrized distribution also contains the factor 1/2 in the cross section.

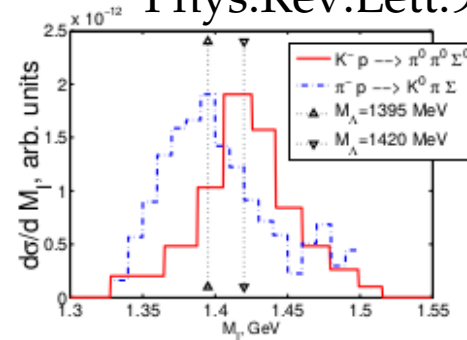
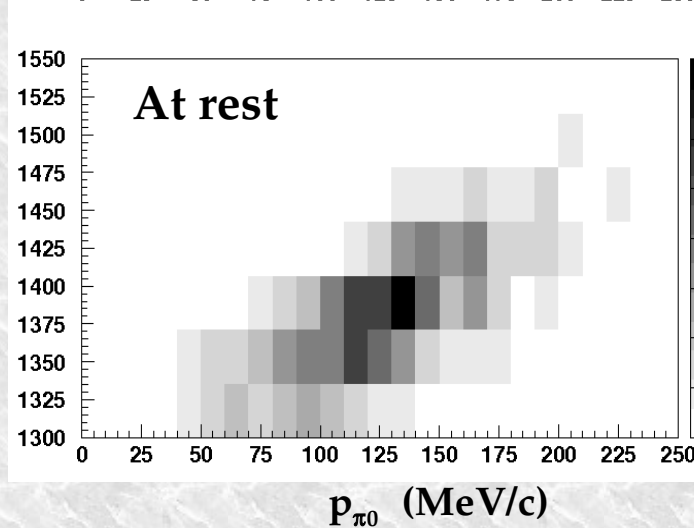
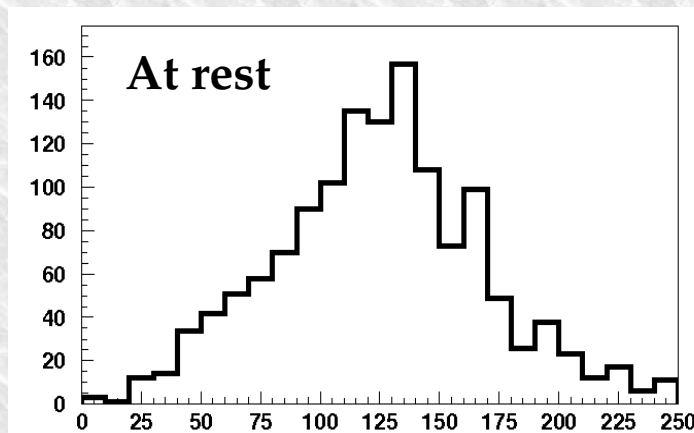
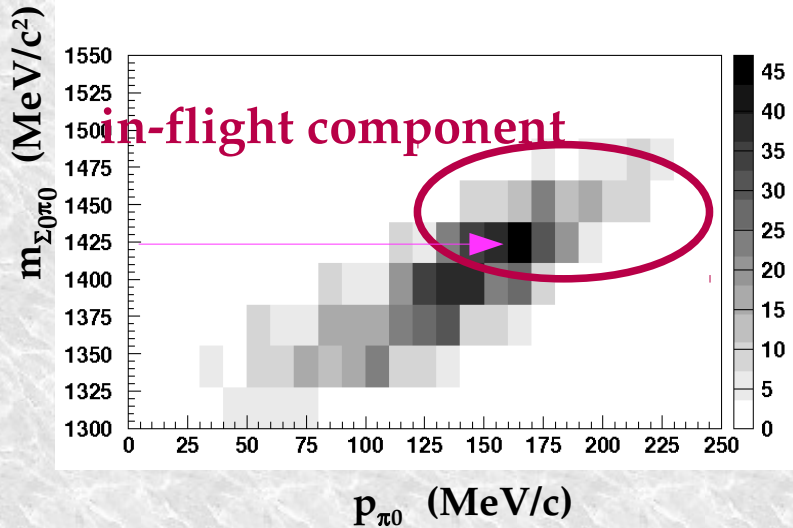
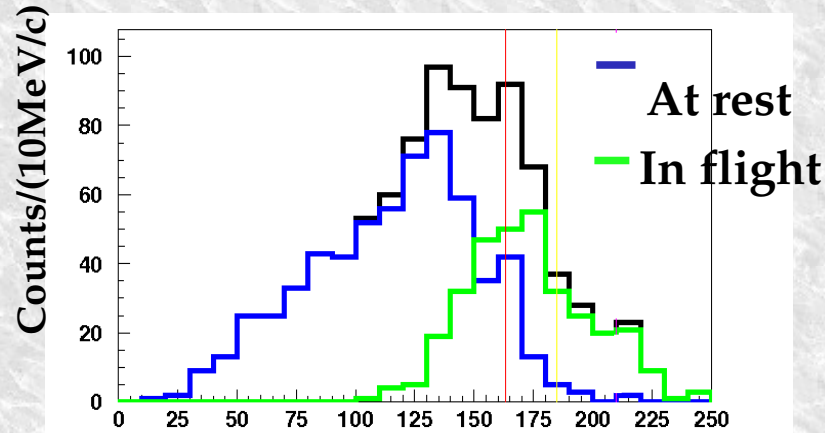


FIG. 5: Two experimental shapes of $\Lambda(1405)$ resonance. See text for more details.

p_{π^0} resolution: $\sigma_p \approx 12 \text{ MeV}/c$



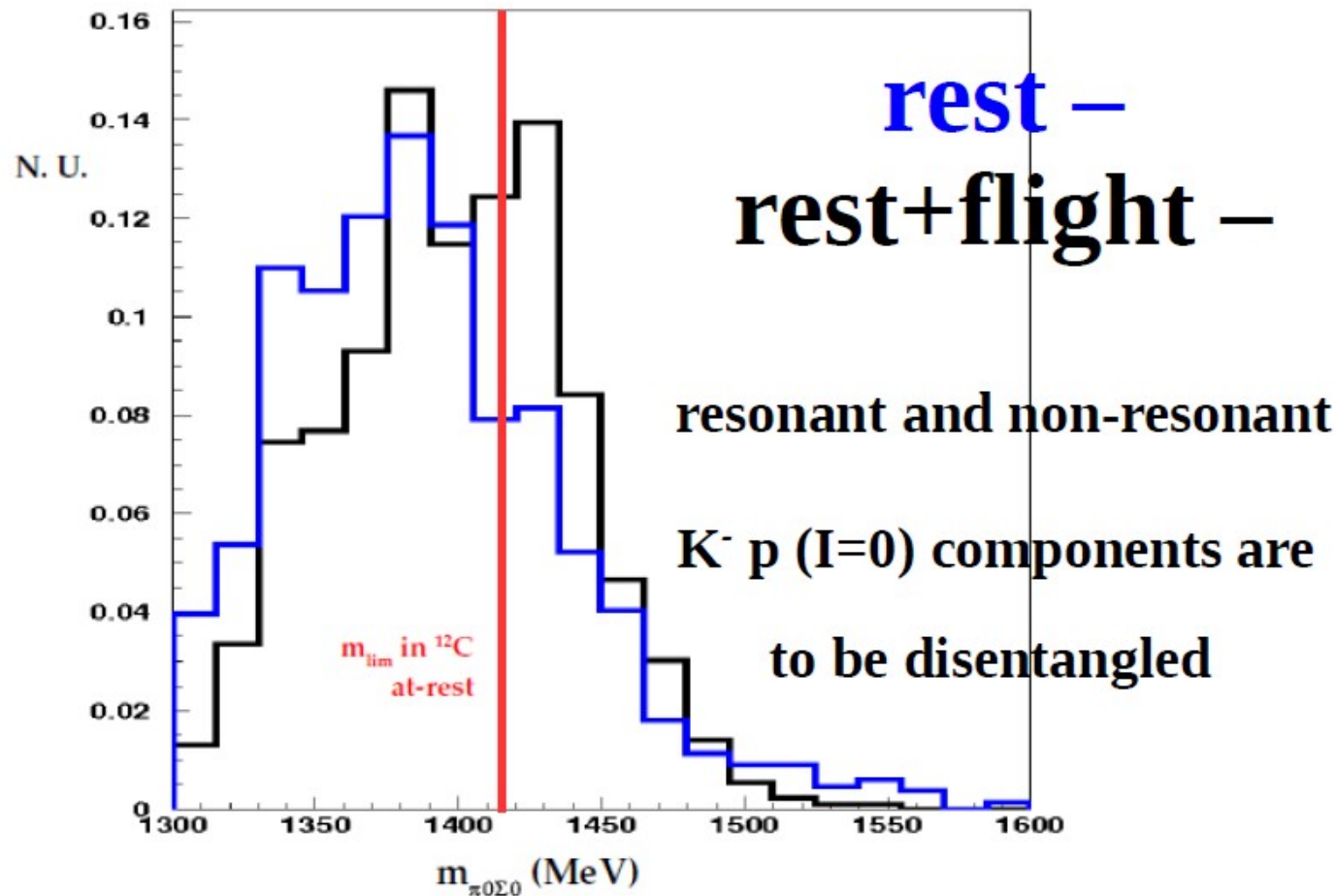
IN-FLIGHT
K-12C
 opens a window
 between 1416 MeV
 and K-Nth

$\Lambda(1405)$: extracting the resonant $I = 0$ contribution

PID optimised, data fit is ongoing

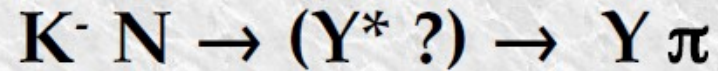
necessary the input of the $\Lambda\pi^-$ measurement

- K. Piscicchia et al., APP B48 (2017) 10, 1875
- C. Curceanu, K. Piscicchia et al., APP B46 (2015) 1, 203



IN-FLIGHT
K- ^{12}C
opens a window
between 1416 MeV
and K-Nth

Resonant VS non-resonant



how much comes from resonance ?

Non resonant transition amplitude

never measured before below threshold

can be obtained exploiting $K^- N$ in-medium absorption,

chosen target ${}^4\text{He}$

- K^- angular momentum at the capture
 - absorbing nucleon wave function
- } known quantities

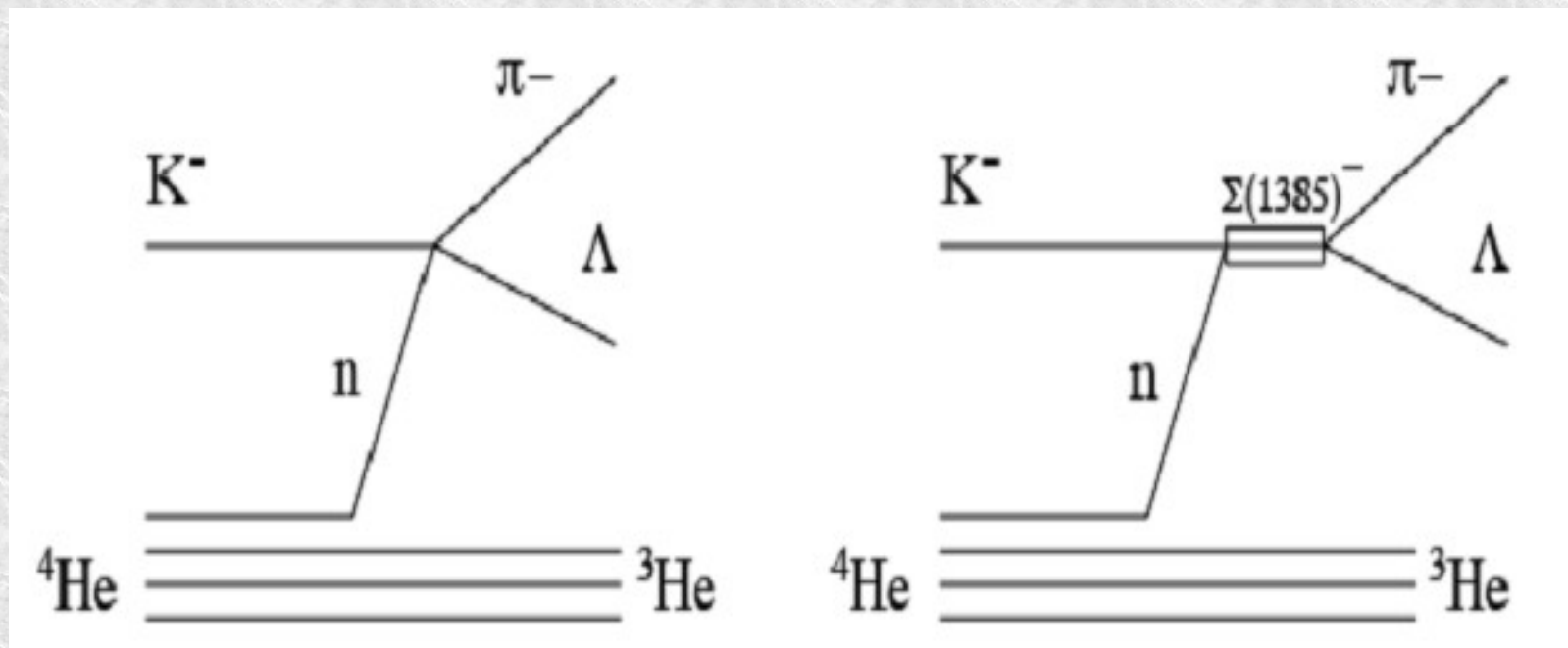
Resonant VS non-resonant

Investigated using:

$K^- "n" \rightarrow \Lambda \pi^-$ direct formation in ${}^4\text{He}$

the goal is to measure $|f^{\text{N-R}}_{\Lambda\pi}(\mathbf{I}=1)|$

to get information on $|f^{\text{N-R}}_{\Sigma\pi}(\mathbf{I}=0)|$



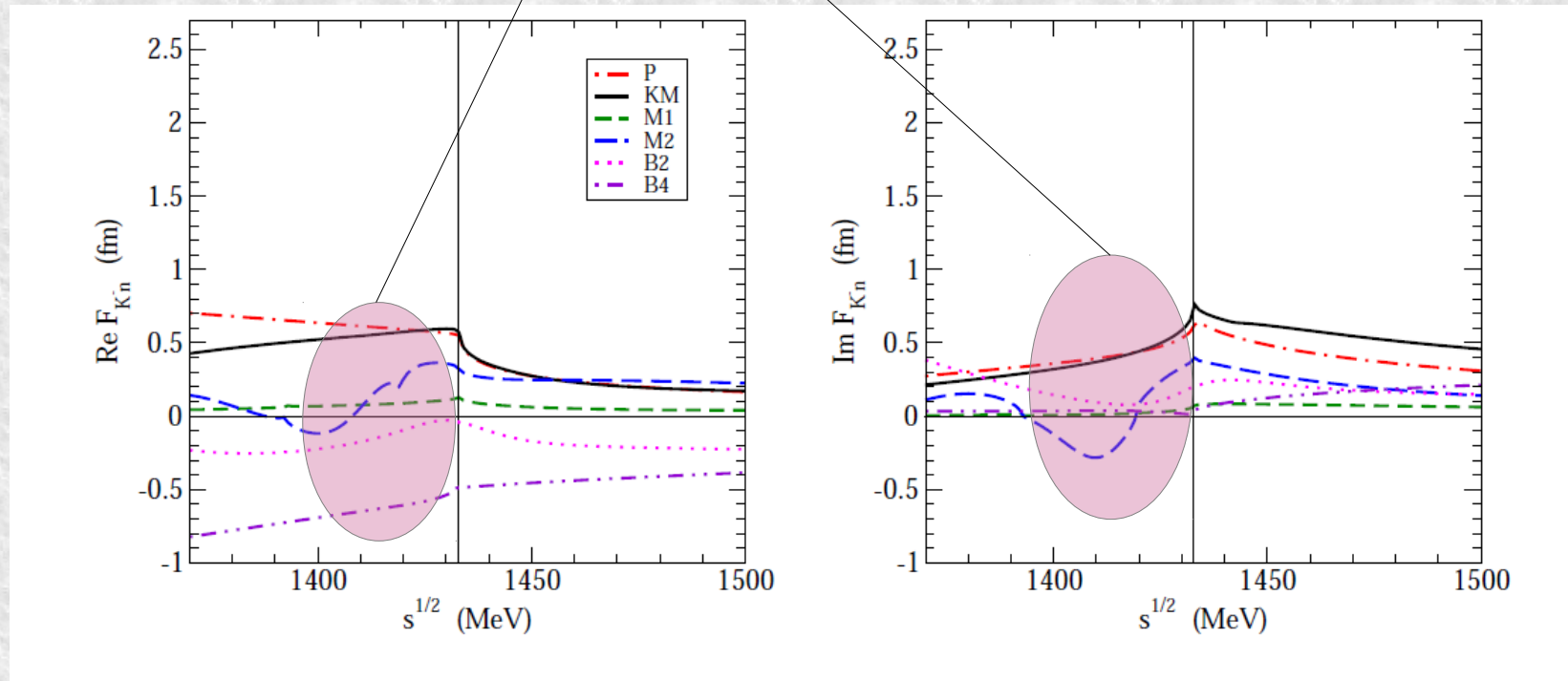
Resonant VS non-resonant

Investigated using:

$K^- "n" \rightarrow \Lambda \pi^-$ to extract $|f_{\Lambda\pi}^{N-R}(I=1)|$
below threshold

J. Hrtankova, and J. Mares, Phys. Rev. C96, (2017) 015205

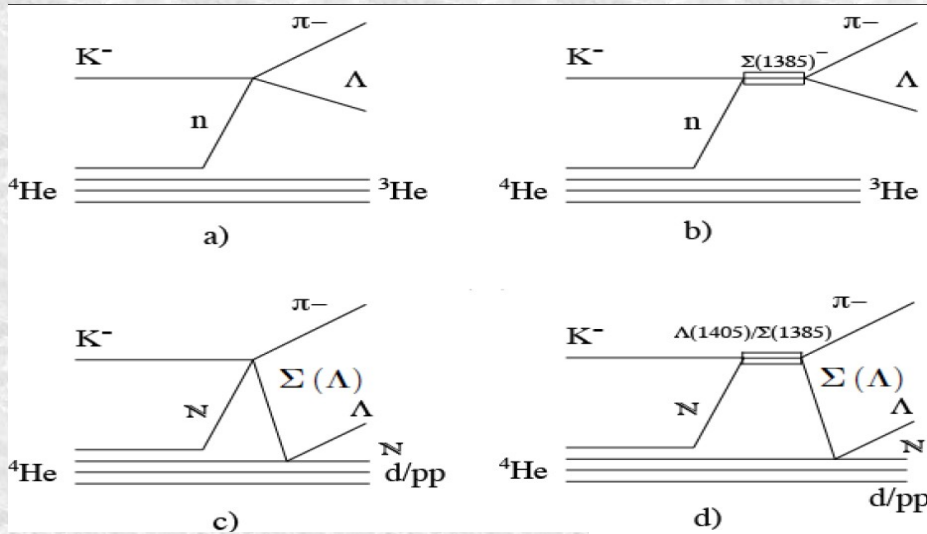
A. Cieply et al., Nucl. Phys. A954, (2016) 17



$K^- \ ^4\text{He} \rightarrow \Lambda p^- \ ^3\text{He}$ resonant and non-resonant processes

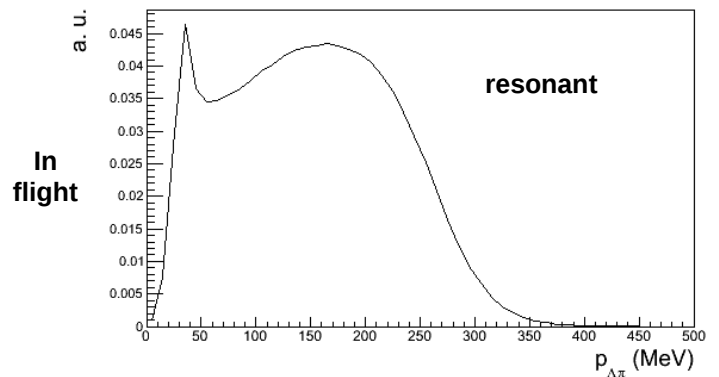
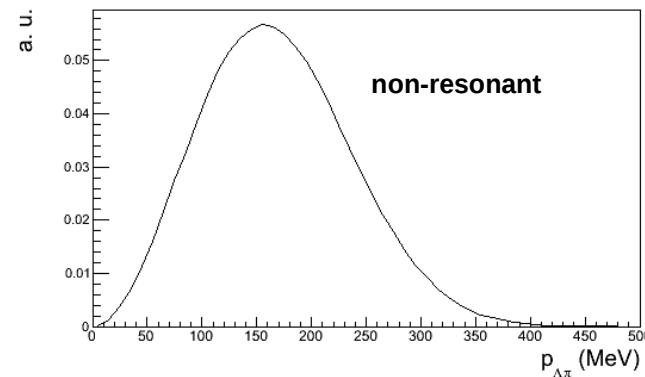
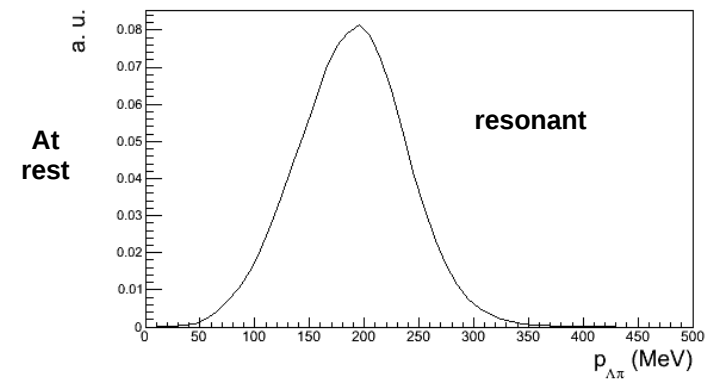
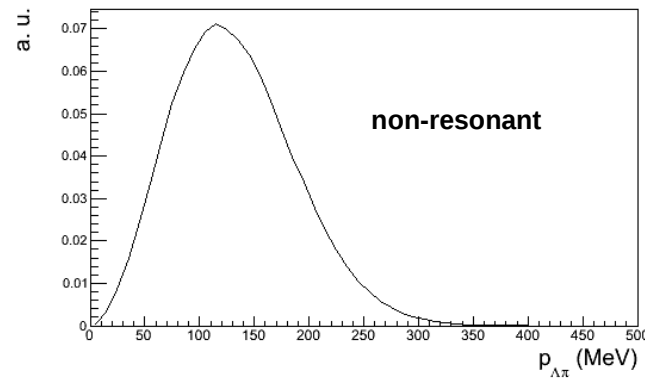
K. P., S. Wycech and C. Curceanu, Nucl. Phys. A954 (2016) 75-93

R. Del Grande, K. P., S. Wycech, Acta Phys. Pol. B 48 (2017) 1881

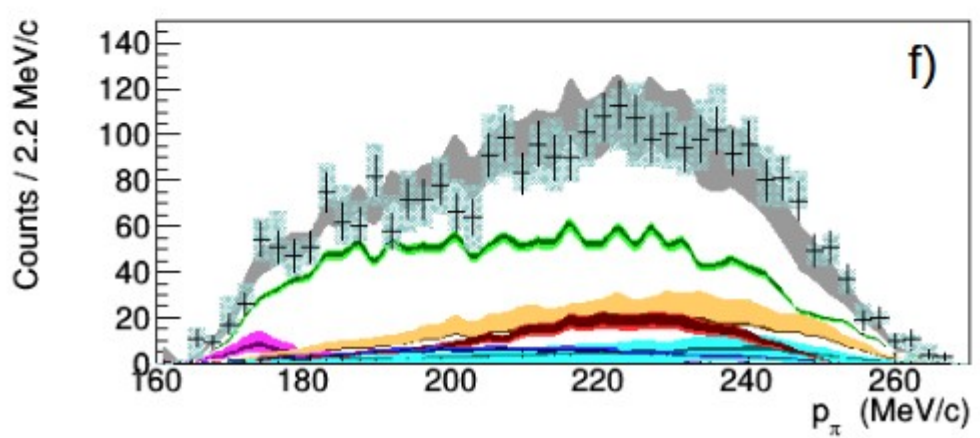
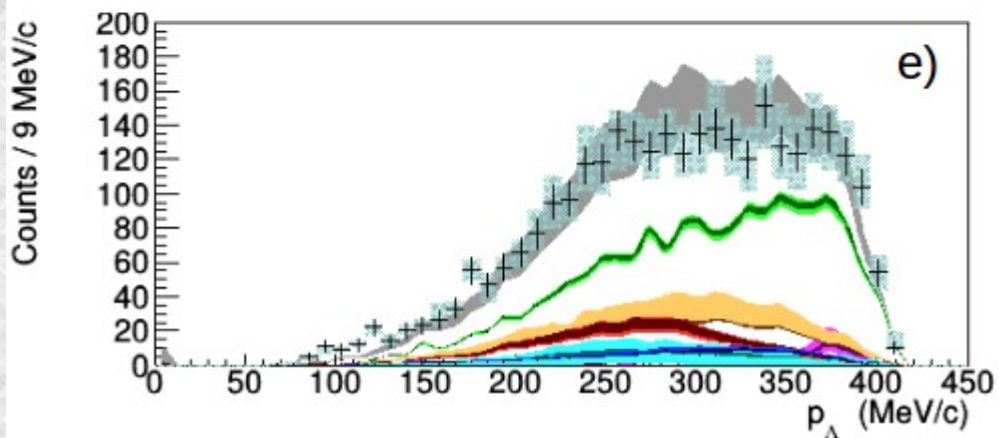
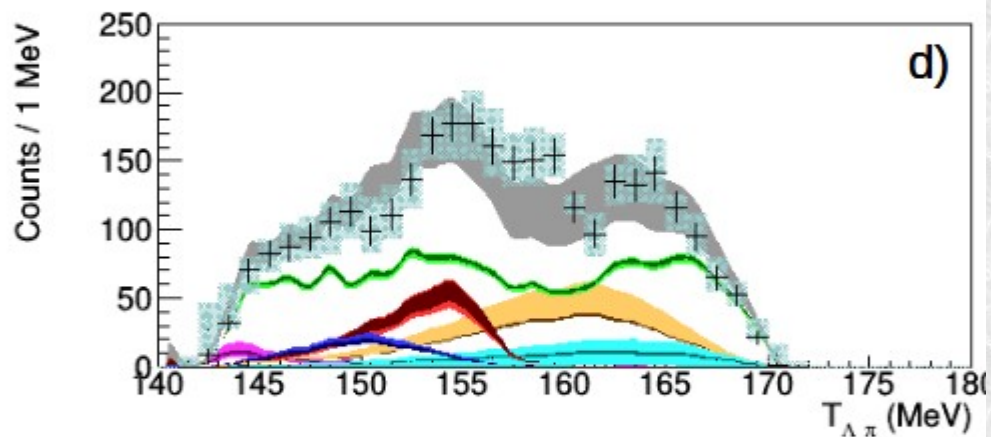
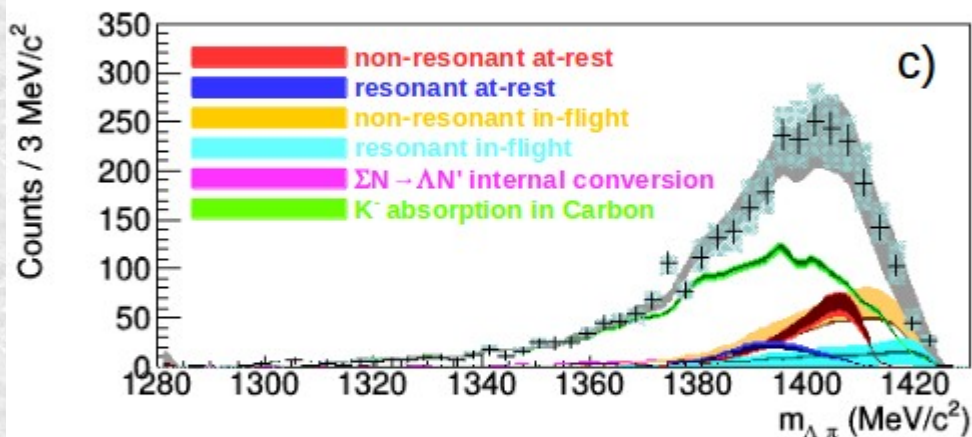
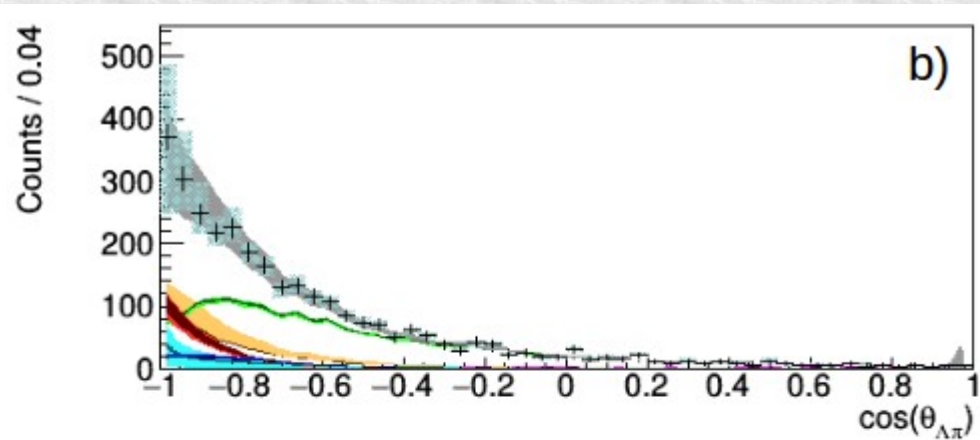
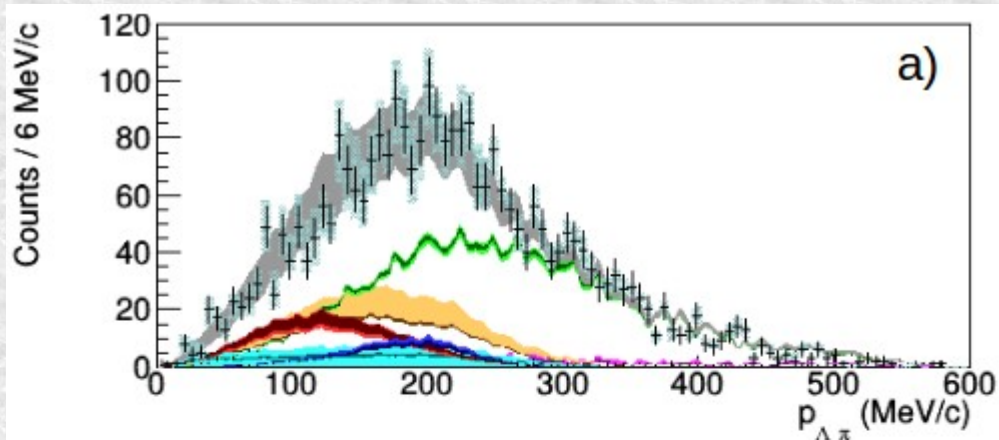


Theoretical shapes for :

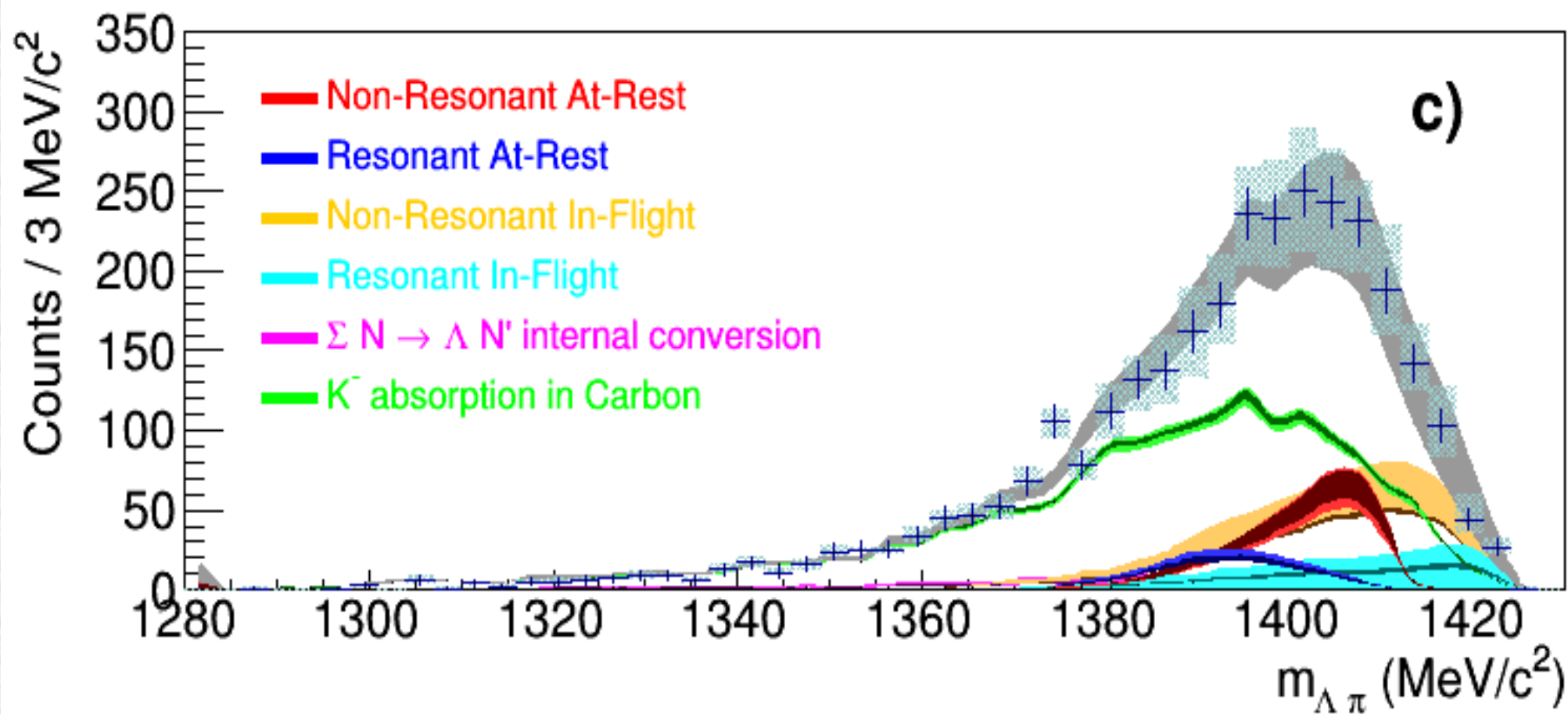
total $\Lambda\pi^-$ momentum spectra for the resonant (Σ^{*-}) and non-resonant ($l = 1$) processes were calculated, for both S-state and P-state K^- capture at-rest and in-flight. Corrections to the amplitudes due to Λ/π final state interactions were estimated.



Simultaneous fit : $(p_{\Lambda\pi^-} - m_{\Lambda\pi^-} - \cos(\theta_{\Lambda\pi^-}))$



Comparison



$m_{\Lambda\pi}$ fit

Light band sys err.
Dark band stat. Err.

Outcome of the measurement

From the well known Σ^* transition probability:

$$\frac{\text{NR} - \text{ar}}{\text{RES} - \text{ar}} = \frac{\int_0^{p_{max}} P_{ar}^{nr}(p_{\Lambda\pi}) dp_{\Lambda\pi}}{\int_0^{p_{max}} P_{ar}^{res}(p_{\Lambda\pi}) dp_{\Lambda\pi}} =$$

$$= |f_{ar}^s|^2 \cdot 8,94 \cdot 10^5 \text{MeV}^2 .$$



$$|f_{ar}^{nr}| = |A_{K^- n \rightarrow \Lambda \pi^-}| = (0.334 \pm 0.018 \text{ stat}_{-0.058}^{+0.034} \text{ syst}) \text{ fm}$$

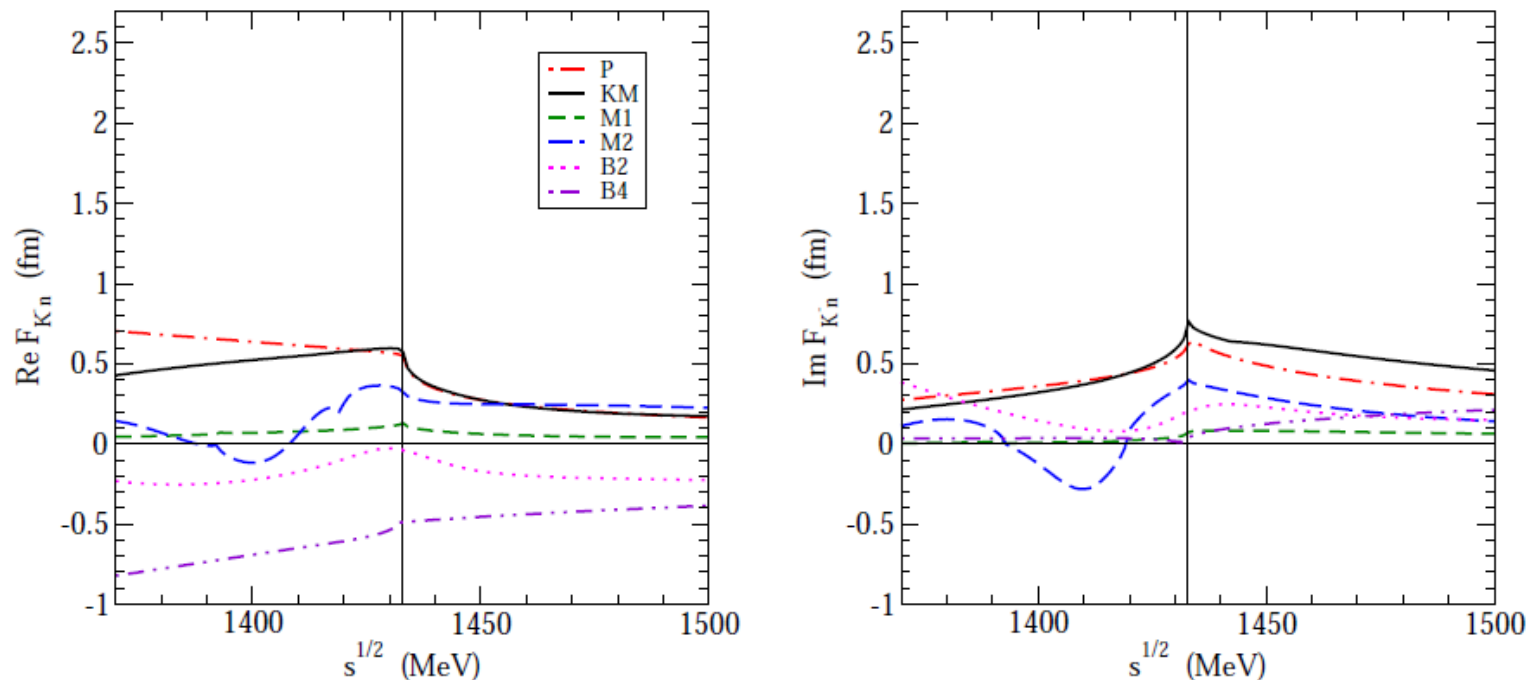
compatible with $K^- p \rightarrow \Lambda \pi^0$ scattering above threshold

J. K. Kim, Columbia University Report, Nevis 149 (1966),

J. K. Kim, Phys Rev Lett, 19 (1977) 1074:

$E = -33 \text{ MeV}$	$p_{lab} = 120 \text{ MeV}$	160 MeV	200 MeV	245 MeV
$0.334 \pm 0.018 \text{ stat}_{-0.058}^{+0.034} \text{ syst}$	0.33(11)	0.29(10)	0.24 (6)	0.28(2)

Outcome of the measurement



To compare with theoretical calculations:

- 1) extract the amplitude for each model .. $A_{K-n} = (\text{Re}F_{K-n}^2 + \text{Im}F_{K-n}^2)^{1/2}$
- 2) scale the amplitudes for the $K^- n$ couplings to the $\Sigma^-\pi^0$ and $\Sigma^0\pi^-$ channels:

$$\frac{\text{Prob}_{K^-n \rightarrow \Lambda\pi^-}}{\text{Prob}_{K^-n \rightarrow \Sigma^-\pi^0}} = \frac{Ph_{K^-n \rightarrow \Lambda\pi^-}}{c_1 Ph_{K^-n \rightarrow \Sigma^-\pi^0}}$$

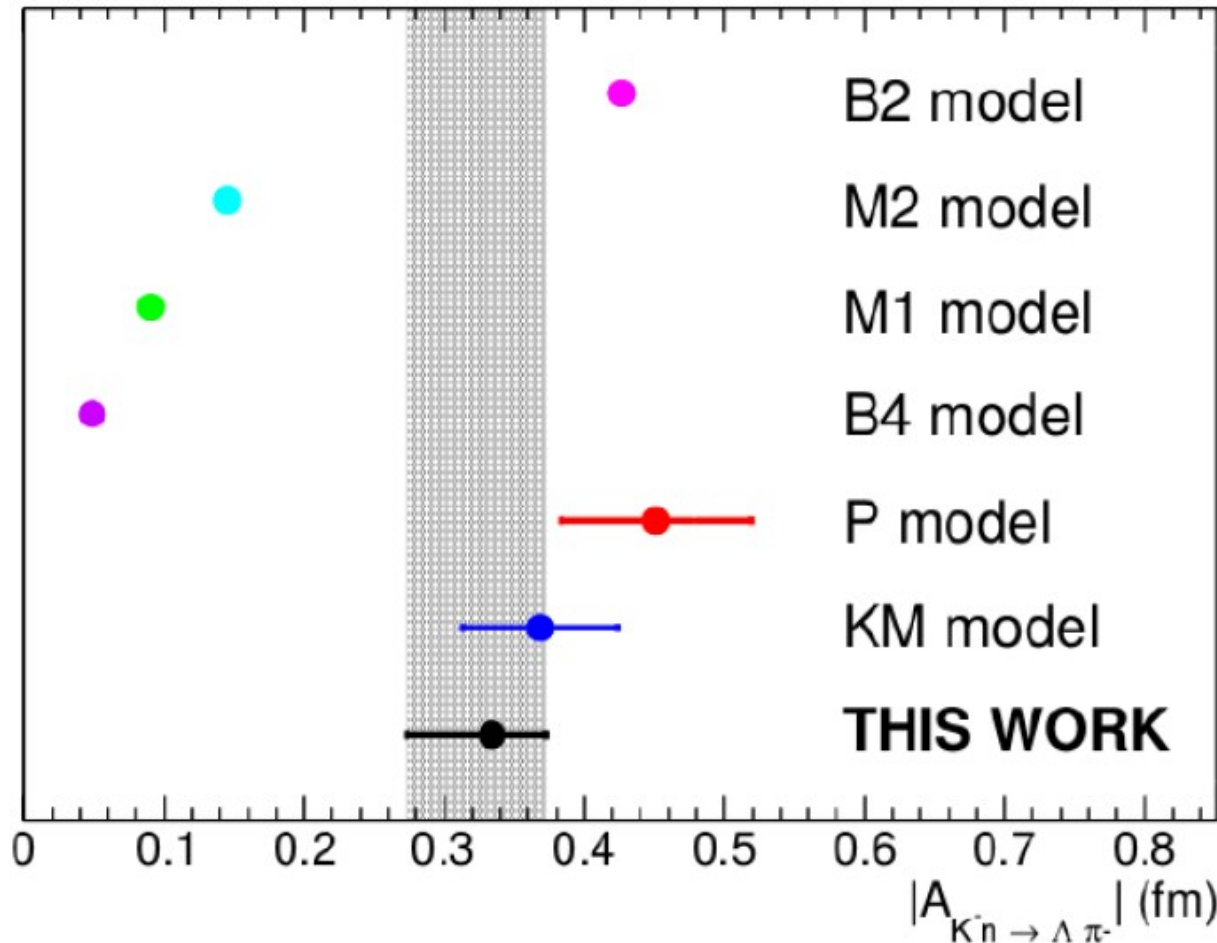
Isospin $(I, I_z) =$
 $= (1, -1)$ component

$$\frac{\text{Prob}_{K^-n \rightarrow \Lambda\pi^-}}{\text{Prob}_{K^-n \rightarrow \Sigma^0\pi^-}} = \frac{Ph_{K^-n \rightarrow \Lambda\pi^-}}{c_2 Ph_{K^-n \rightarrow \Sigma^0\pi^-}}$$

Phase spaces ratios

Outcome of the measurement

$$|f_{ar}^s| = (0.334 \pm 0.018 \text{ stat}_{-0.058}^{+0.034} \text{ syst}) \text{ fm}.$$



$$A_{K^- n \rightarrow \Lambda \pi^-} (s^{1/2} \sim 1400 \text{ MeV})^{1/2}$$

$$E_{K^- n} = -|B_n| - \frac{p_3^2}{2\mu_{\pi, \Lambda, 3He}}$$

Nucl. Phys. A954 (2016) 75-93

Phys. Rev. C 96 (2017) 045204

Phys. Lett. B 702 (2011) 402-407

Nucl.Phys. A968 (2017) 35-47

K. P., S. Wycech, L. Fabbietti et al. Phys.Lett. B782 (2018) 339-345

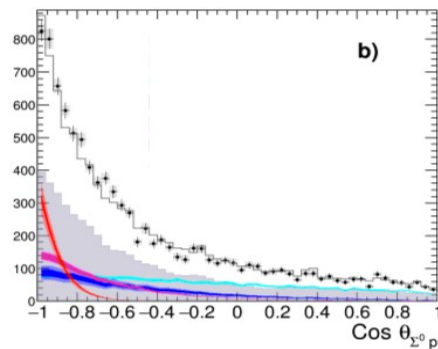
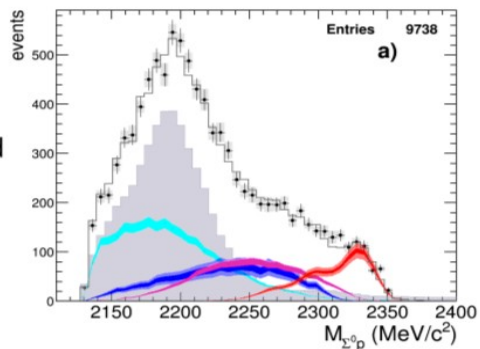
K⁻ - multiN absorption and search for bound states

AMADEUS contribution from low energy K^- ^{12}C absorption $\Sigma^0_p / \Lambda p$ final states

O. Vazquez Doce et al, Phys Lett B 758, (2016) 134

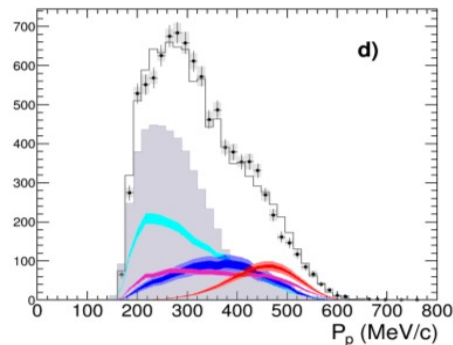
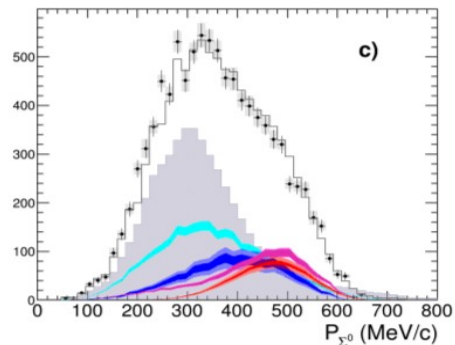
Final fit

- data
- π^0 background
- 4NA+Uncorr.
- 3NA
- 2NA FSI
- 2NA QF
- Total fit



$$\chi^2 = 0.85$$

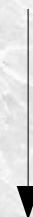
2NA-QF clearly separated from other processes



From the contributions to the fit, the yields are extracted for K- stop

	yield / $K^-_{stop} \cdot 10^{-2}$	$\sigma_{stat} \cdot 10^{-2}$	$\sigma_{syst} \cdot 10^{-2}$
2NA-QF	0.127	± 0.019	+0.004 -0.008
2NA-FSI	0.272	± 0.028	+0.022 -0.023
Tot 2NA	0.376	± 0.033	+0.023 -0.032
3NA	0.274	± 0.069	+0.044 -0.021
Tot 3body	0.546	± 0.074	+0.048 -0.033
4NA + bkg.	0.773	± 0.053	+0.025 -0.076

no significant bound state emerges at the level of 2σ



– Λp analogous analysis finalized

- K-multi-nucleon yields & cross sections obtained for $p_K \sim 100$ MeV/c

- disappearance of the bound state in K^- ^{12}C induced reaction explained

K⁻ - 4NA cross section & BR

At available data

Available data:

- in Helium :

- bubble chamber experiment

[M.Roosen, J.H. Wickens, Il Nuovo Cimento 66, (1981), 101]

K⁻ stopped in liquid helium, Λ dn/t search. **3 events** compatible with the At kinematics were found

$$\text{BR}(K^{-4}\text{He} \rightarrow \Lambda t) = (3 \pm 2) \times 10^{-4} / K_{\text{stop}} \quad \text{global, no 4NA}$$

- Solid targets

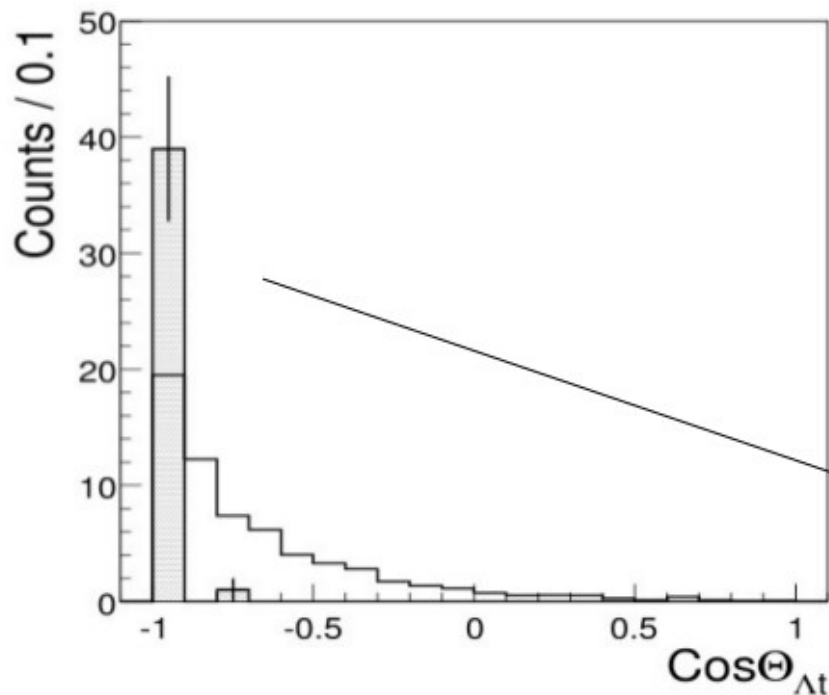
- FINUDA [Phys.Lett. B669 (2008) 229]

(**40 events** in different solid targets)

Λt available data

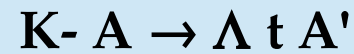
FINUDA presented [Phys.Lett.B (2008) 229]:

- a study of Λ vs t momentum correlation and an opening angle distribution
- **40 events** collected and added together coming from different targets (${}^6,7\text{Li}$, ${}^9\text{Be}$)



Filled histogram= data

Open histogram = Phase space simulation



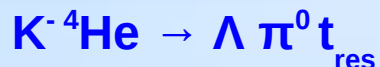
Unclear back to back topology

Λt emission yield $\rightarrow 10^{-3} - 10^{-4} / K^-_{\text{stop}}$
global, no 4NA

Experimental data only back-to-back

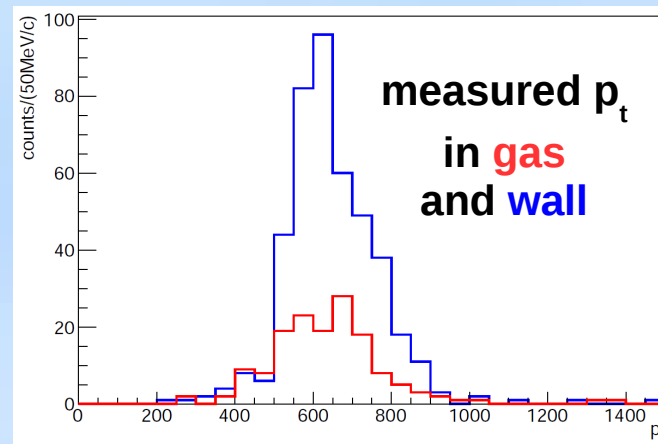
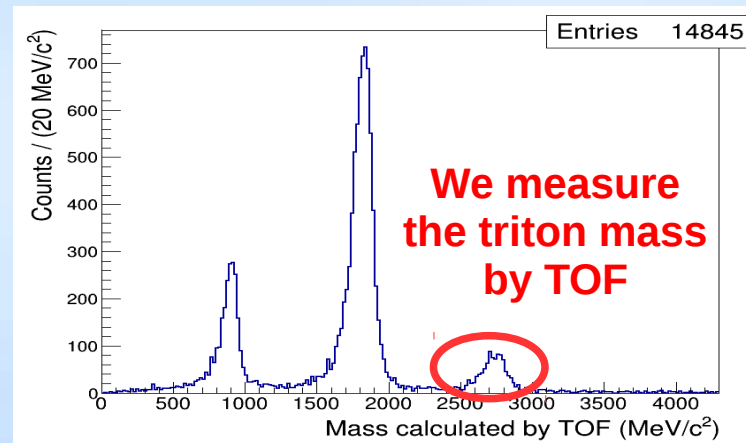
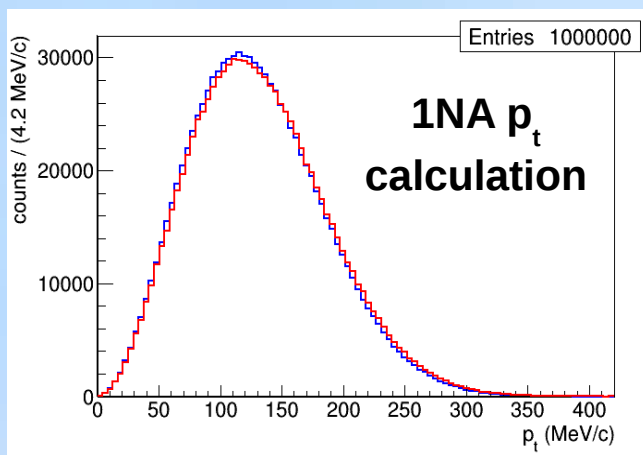
$K^- \ ^4\text{He} \rightarrow \Lambda t$ cross section, DC gas sample contributing processes:

single nucleon absorption (1NA)



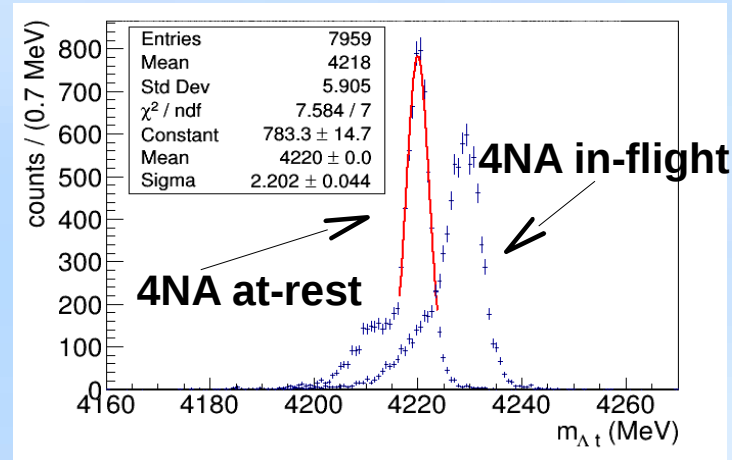
Spectator tritons have low momentum:

$p_t \sim$ Fermi momentum



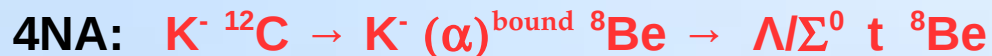
4NA processes – K^- absorbed on FREE α :

- $K^- \ ^4\text{He} \rightarrow \Lambda t$
- $K^- \ ^4\text{He} \rightarrow \Sigma^0 t, \quad \Sigma^0 \rightarrow \Lambda \gamma$



$K^- \ ^4\text{He} \rightarrow \Lambda t$ cross section, DC gas sample contributing processes:

Main background: K^- absorption on ^{12}C (isobutane contamination)



7 MeV/c^2 lower invariant mass threshold respect to:

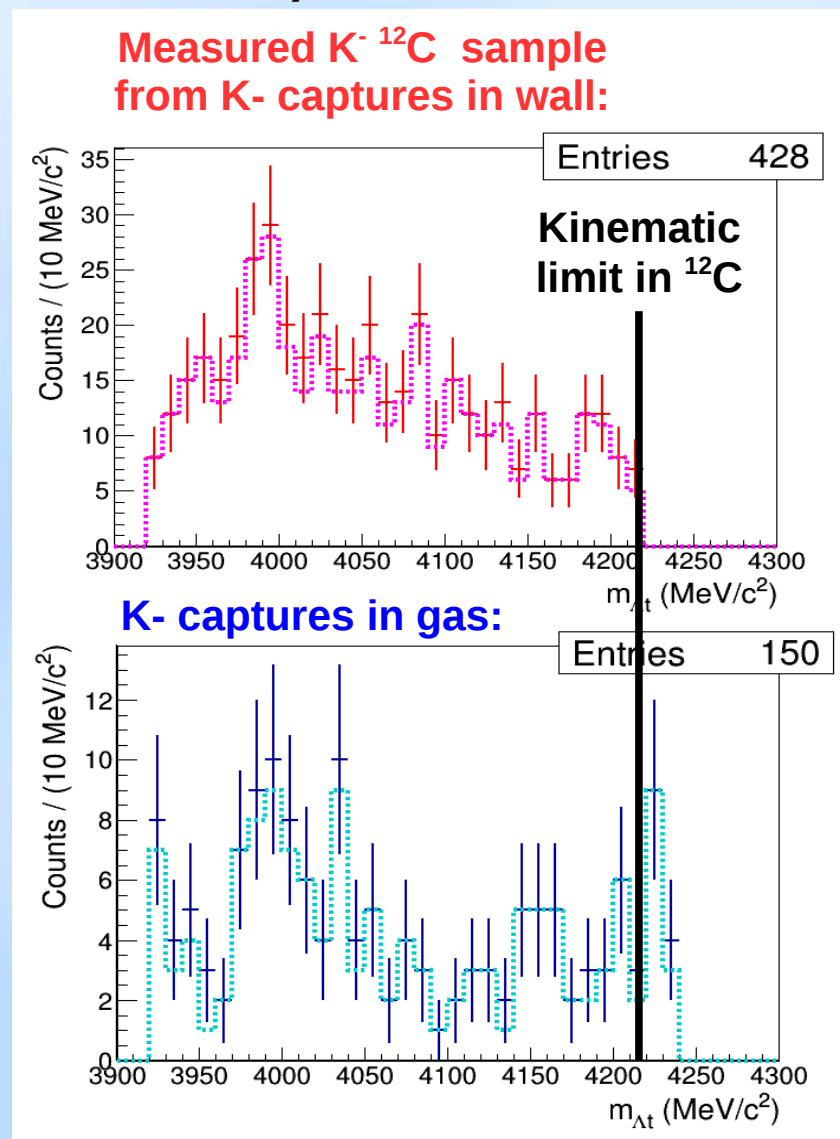
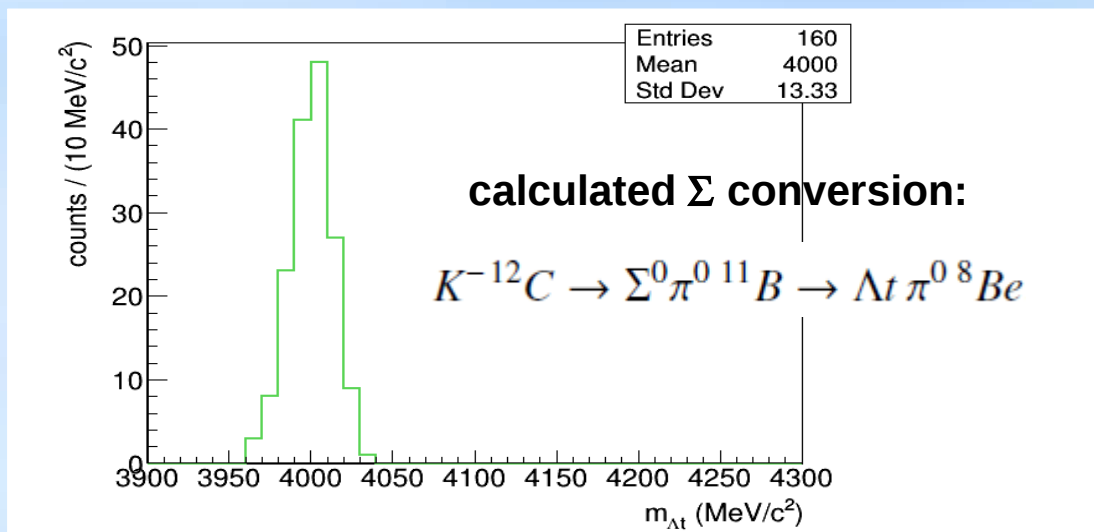


+

all possible elastic/inelastic FSI processes with primary Λ/Σ formation



uncorrelated Λt low invariant mass:



$K^- \text{ } ^4\text{He} \rightarrow \Lambda t$ 4NA fit

preliminary

+ data

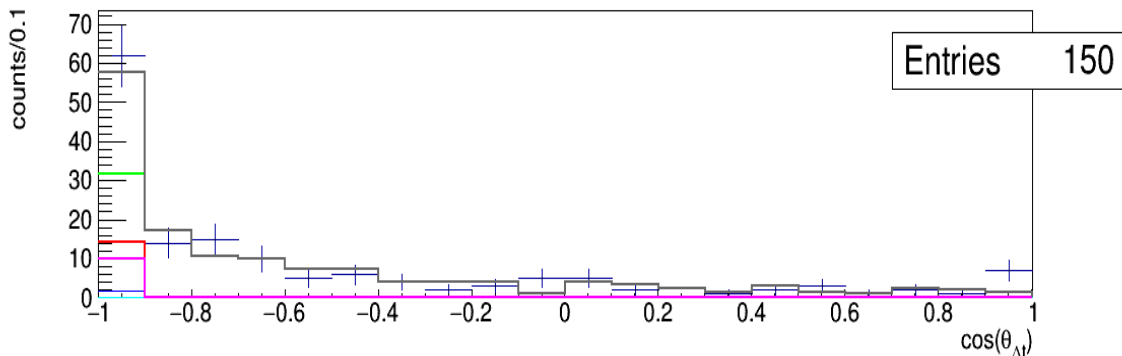
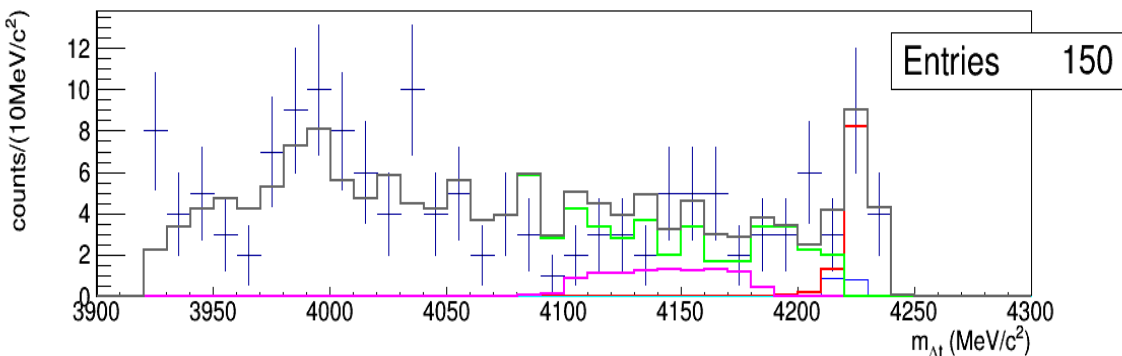
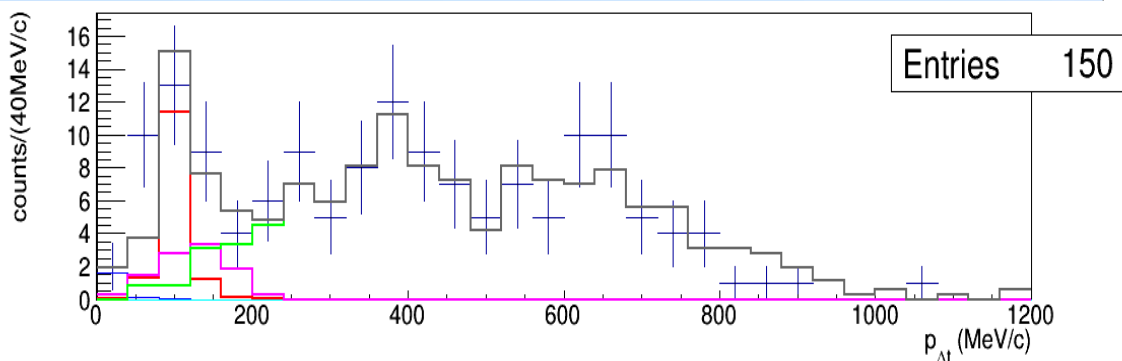
--- carbon data from DC wall

--- 4NA $K^- \text{ } ^4\text{He} \rightarrow \Lambda t$ in flight MC

--- 4NA $K^- \text{ } ^4\text{He} \rightarrow \Lambda t$ at rest MC

--- 4NA $K^- \text{ } ^4\text{He} \rightarrow \Sigma^0 t$, $\Sigma^0 \rightarrow \Lambda \gamma$ MC

--- 4NA $K^- \text{ } ^4\text{He} \rightarrow \Sigma^0 t$, $\Sigma^0 \rightarrow \Lambda \gamma$ MC

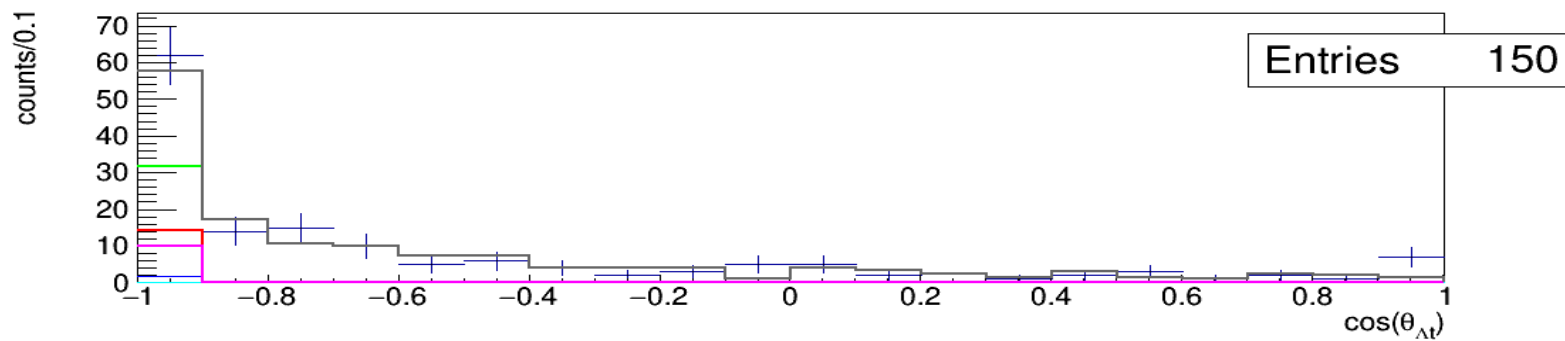
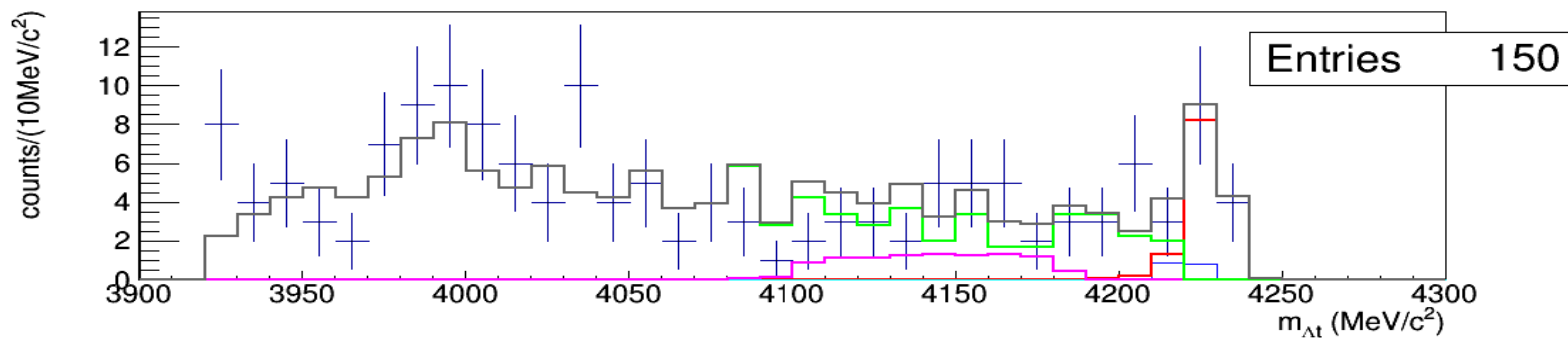
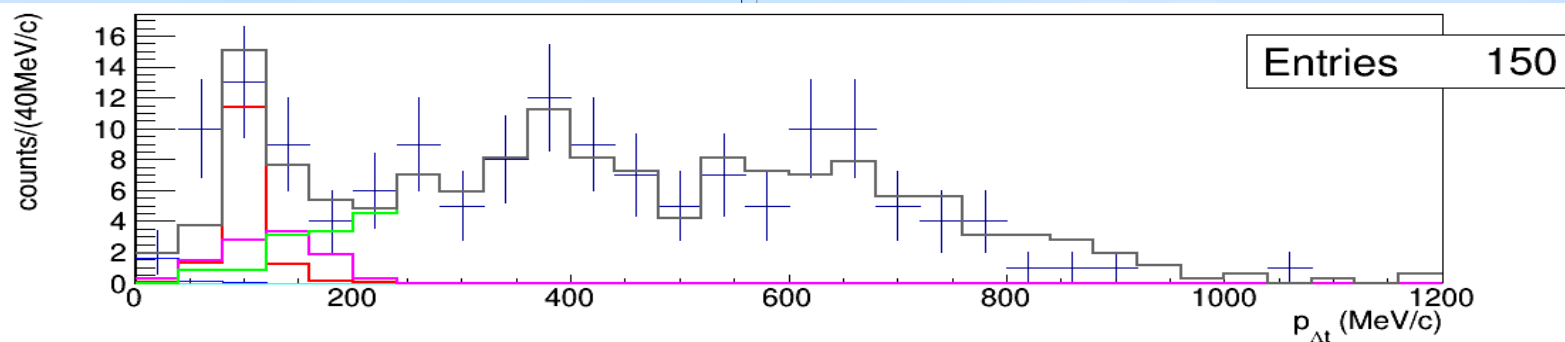


K-⁴He → Λt 4NA fit

preliminary

$$\text{BR}(\text{K}^4\text{He}(4\text{NA}) \rightarrow \Lambda t) < 2.0 \times 10^{-4} / K_{\text{stop}} \quad (95\% \text{ c. l.})$$

$$\sigma(100 \pm 19 \text{ MeV}/c) (\text{K}^4\text{He}(4\text{NA}) \rightarrow \Lambda t) = \\ = (0.81 \pm 0.21 \text{ (stat)}^{+0.03}_{-0.04} \text{ (syst)}) \text{ mb}$$



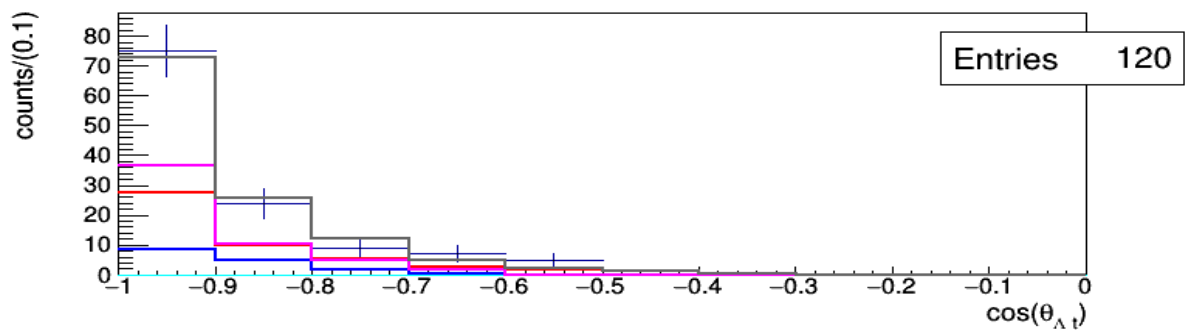
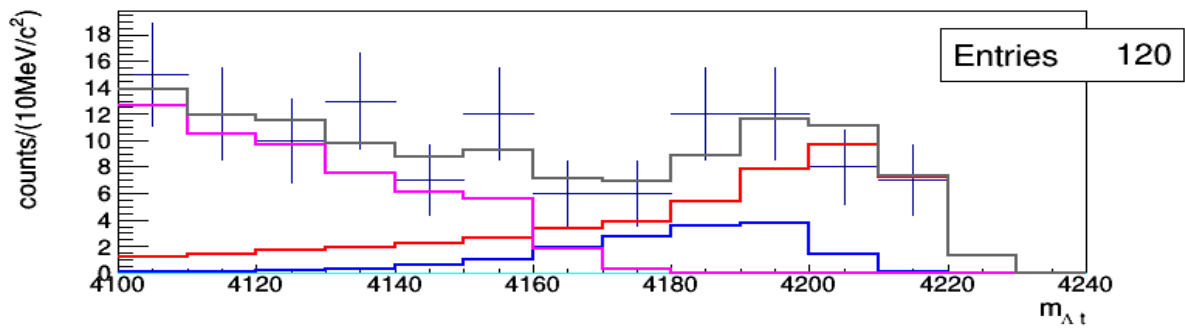
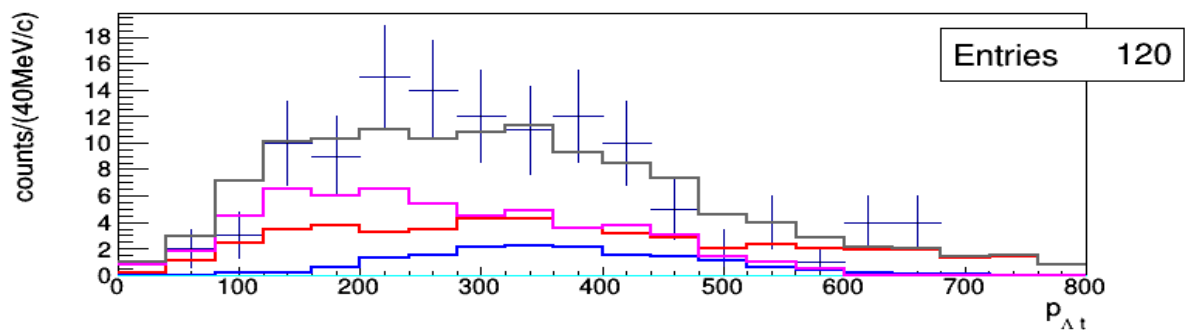
$K^- ^{12}\text{C} \rightarrow \Lambda/\Sigma^0 t \text{ } ^8\text{Be}$ 4NA without FSI

$$\text{BR}(K^- ^4\text{He}(4\text{NA}) \rightarrow \Lambda t) = 1.5 \pm 0.5 \times 10^{-4} \text{ (stat) } /K_{\text{stop}}$$

$$\sigma(K^{12}\text{C} (4\text{NA}) \rightarrow \Lambda t \text{ } ^8\text{Be}) = 0.58 \pm 0.11 \text{ (stat) mb}$$

$$\sigma(K^{12}\text{C} (4\text{NA}) \rightarrow \Sigma^0 t \text{ } ^8\text{Be}) = 1.88 \pm 0.35 \text{ (stat) mb}$$

preliminary

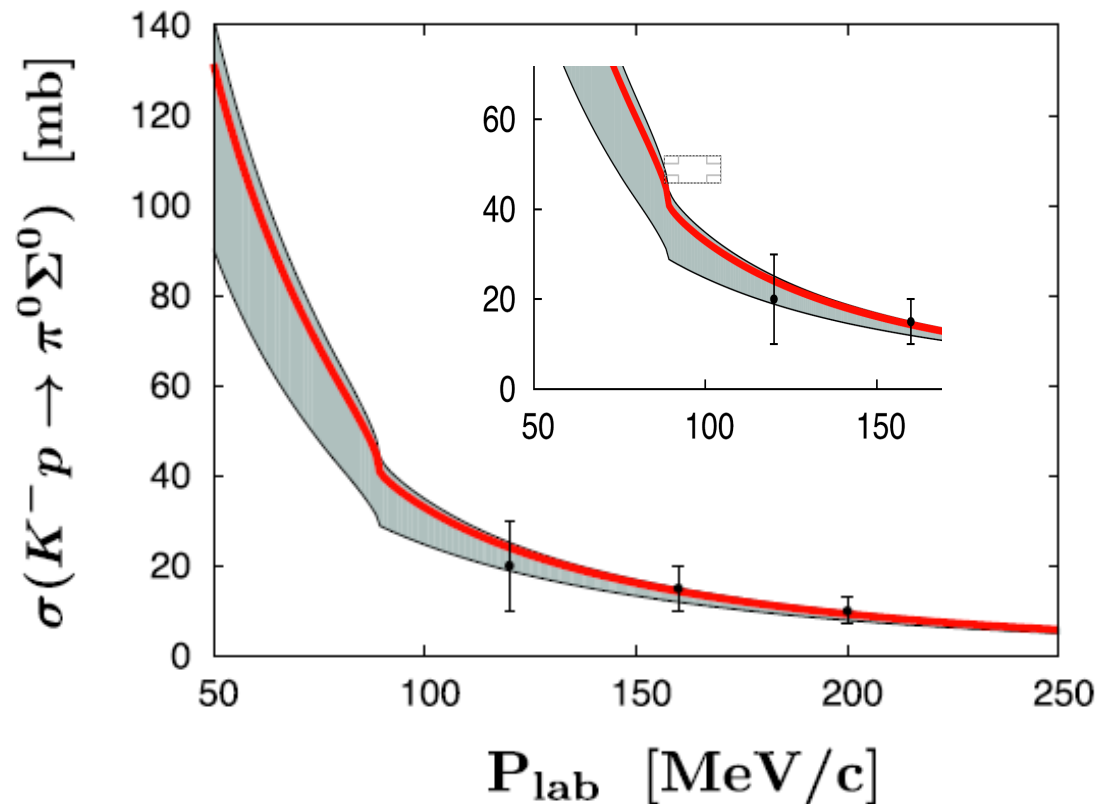


Perspective:

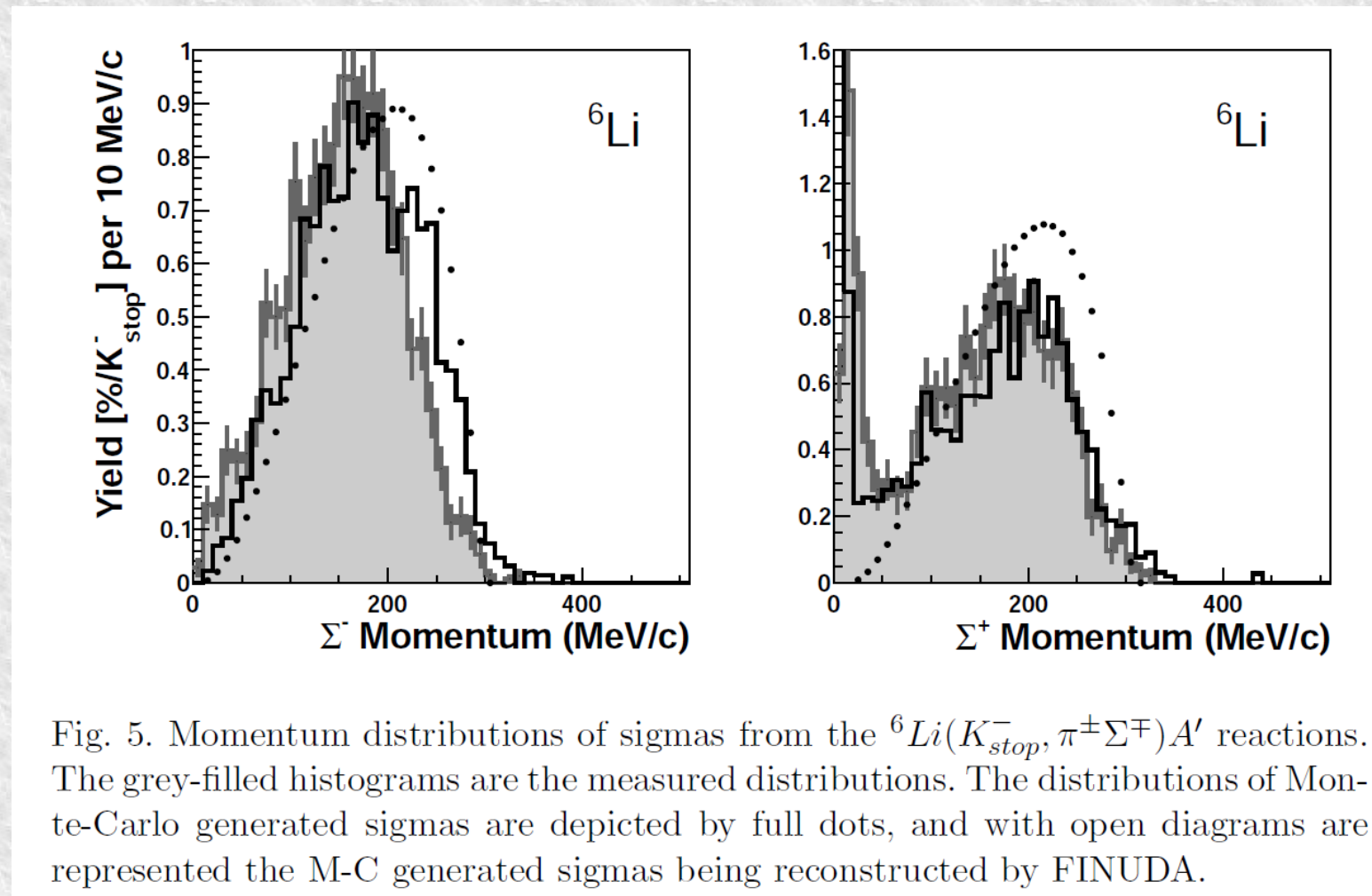
Measurement of the

$K^- p \rightarrow \Sigma^0 \pi^0$ cross section for $p_K = 97 \pm 10$ MeV/c

Y. Ikeda, T. Hyodo, W. Weise,
PLB 706, 63 (2011); NPA 881 98 (2012)



Low momentum p_{Σ^+} structure in $\Sigma^+\pi^-$ formation

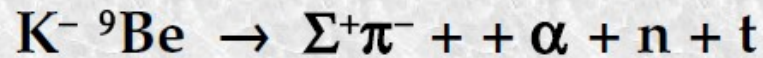


FINUDA coll. M. Agnello et al., Phys. Lett. B704 (2011) 474.

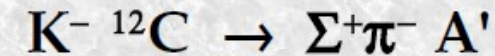


Low momentum p_{Σ^+} structure in $\Sigma^+\pi^-$ formation

K. Piscicchia et al., EPJ Web Conf. 137 (2017) 09005.



no structure at low momentum



structure at low momentum

amounts some % of the total yield

also in thinner targets

(not explained by energy loss)

Hypothesis: Σ^+ trapped in a Gamov state, interplay of the attractive nuclear potential & repulsive Coulomb barrier

S. Wycech, K. P., EPJ Web. Conf. 130 (2016) 02011

R. Del Grande, K. P. and S. Wycech, Acta Phys.Polon. B48 (2017) 1881

S. Wycech, K. P., On Gamov states of Σ^+ hyperons, Acta Phys.Polon. B48 (2017) 1861

Gamov state formation of a Σ^+ in light nuclei?

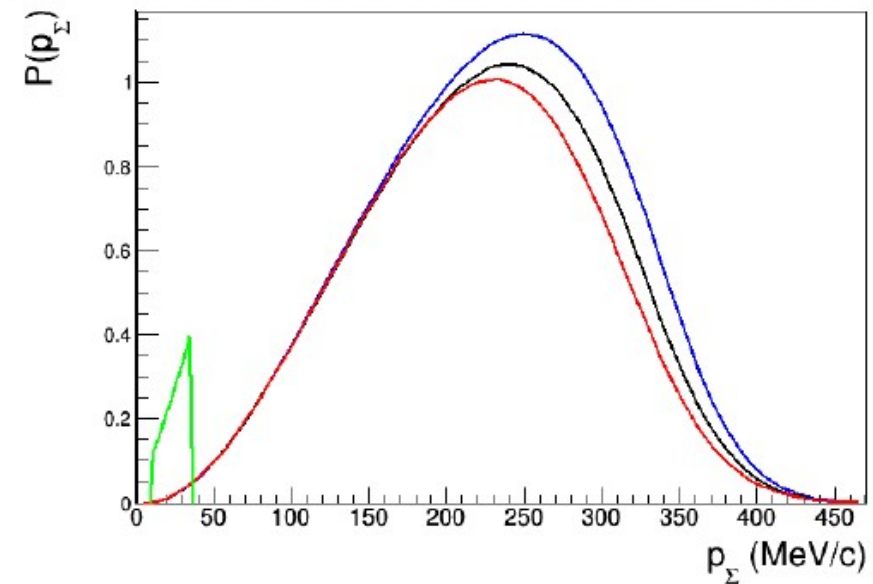
... work in progress

Gamov peak following in-flight capture

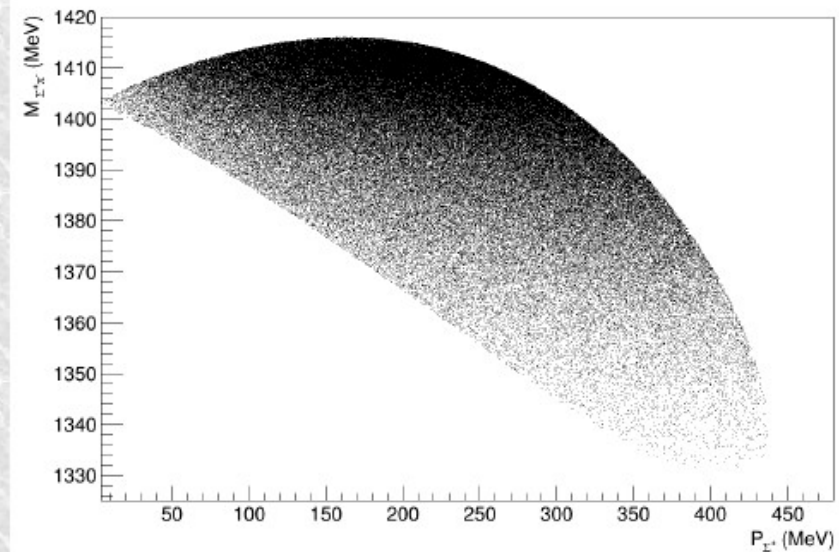


about 3% of the large peak

Breit – Wigner - $(E, \Gamma) = (1405, 40) ; (1410, 40) ;$
 $(1420, 40)$



Position $p_{\Sigma^+} = 15 \text{ MeV}/c$
peculiar structure due to
the limitation of the phase space



Thank you